AMPK-mediated mTORC1 regulation in macrophage metabolism and polarization

Victoria Robert-Gostlin

Thesis submitted to the

The Faculty of Medicine

in partial fulfillment of the requirements

for the degree of Master of Science in Biochemistry

July 9th, 2024

Department of Biochemistry, Microbiology, and Immunology

Faculty of Medicine

University of Ottawa

Abstract

The fundamental interplay between immunity and metabolism (immunometabolism) transcends a staggering number of chronic diseases and underpins current and future therapeutic efforts. AMP-activated protein kinase (AMPK) generally promotes catabolic and anti-inflammatory pathways. In contrast, the mechanistic target of rapamycin complex 1 (mTORC1) initiates anabolic and pro-inflammatory pathways. While it is known that AMPK can inhibit mTORC1 activation via two specific targets (Raptor and TSC2), the physiological importance of this signalling axis remains completely unknown. With the help of collaborators, a novel point mutant mouse model where the phosphorylation sites on TSC2 (Ser1387) and Raptor (Ser722/792) have been mutated to alanine (double knock-in mice; DKI) was generated. With these mice, the objective was to map the importance of this signalling axis in macrophage immunometabolism. Using bone marrow-derived macrophages (BMDM) from DKI and wild-type control mice, the lack of phosphorylation of both TSC2 and Raptor was first validated. Moreover, downstream signalling to mTORC1 targets was consistent with a basal increase in mTORC1 activity. Next, macrophages were polarized using validated immune stressors such as bacterial endotoxin and interleukin 4. Changes in metabolic signature and immune responses were assessed by measuring transcript and surface expression markers, expression of metabolic enzymes, and cytokine profiles of these cells. Given that immunometabolism underpins several fundamental macrophage responses, this research seeks to identify how specific metabolic signalling pathways can affect macrophage immune responses in culture to potentially inform how these cells behave under acute and chronic inflammation conditions *in vivo*.

Acknowledgements

I would like to thank my supervisor Dr. Morgan Fullerton for his endless patience and support throughout this thesis. He has taught me an incredible amount over the last two years and has had a significant impact on the scientist I have become. I will always be grateful for his supervision and guidance throughout my master's. It has been a great pleasure being a part of the Immunometabolab and I am immensely grateful for the opportunity to have worked amongst such fantastic scientists. Thank you to Conor, Tyler, Alexia, Madison, Julia and Peyman for their support and expertise throughout this thesis. This thesis would not have been possible without each of my colleagues. I am especially grateful to Peyman for spending countless hours helping me optimize assays and for taking the time to explain many concepts to me throughout this thesis. I am also extremely thankful to my thesis advisory committee Dr. Mary-Ellen Harper and Dr. Ryan Russell for their advice and support. All the people mentioned have played an integral part in helping me get to the end of this thesis, I will be forever thankful for the unwavering support I have received throughout my time at the University of Ottawa.

Table of Contents

List of Tables

List of Figures

Abbreviations

4EBP1 – Eukaryotic translation initiation factor 4E-binding protein 1

Akt – Protein kinase B

AMPK – AMP-activated protein kinase

Arg1 – Arginase 1

BMDM – Bone marrow-derived macrophages

CaMKKβ – Ca2+/Calmodulin-dependent protein kinase kinase β

CHX - Cycloheximide

DAMP – Damage-associated molecular patterns

DEPTOR – DEP domain containing mTOR-interacting protein

DKI – double knock-in

ECAR – Extracellular acidification rate

eFT2 - Eukaryotic elongation factor 2

ETC – Electron transport chain

Fizz1 – Resistin like α

GβL/mLST8 – G protein β-subunit-like/mammalian lethal with Sec13 protein 8

GLUT1 – Glucose transporter protein type I (GLUT1)

HIF-1α – Hypoxia-inducible Factor 1α

HMGCR – 3-hydroxy-3-methyl-glutaryl-coenzyme A reductase

IL – Interleukin

iNOS – Inducible nitric oxide synthase

KI – Knock in

KO – Knock out

LPS – Lipopolysaccharide

LKB1 – Liver kinase B1

mSIN1 – Stress-activated protein kinase-interacting protein 1

mTOR – Mammalian target of rapamycin

mTORC1 – Mammalian target of rapamycin complex 1

mTORC2 – Mammalian target of rapamycin complex 2

NO – Nitric oxide

OCR – Oxygen consumption rate

PAMP – Pathogen-associated molecular patterns

PI3K – Phosphoinositide 3-kinase

PGC1α – Peroxisome proliferator-activated receptor-gamma coactivator 1α

PPP – Pentose phosphate pathway

PRAS40 – Proline-rich AKT substrate of 40 kDa

PRR – Pattern-recognition receptors

PRR5 – Proline-rich 5

Raptor – Regulatory-associated protein of mTOR

Rictor – Rapamycin-insensitive companion of mTOR

S6K – Ribosomal protein S6 kinase

TCA – Tricarboxylic acid

TGF-β – Transforming growth factor-β

TSC2 – Tuberous sclerosis complex 2

TNFα – Tumor necrosis factor α

ULK1 – Unc-51 like autophagy activating kinase 1

WT – Wild-type

YY1 – Ying yang 1

Chapter 1: Introduction

1.1 Macrophage Function

Macrophages are involved in many biological processes, including tissue homeostasis, repair, and pathogen response. These tissue-resident innate immune cells are professional phagocytes, meaning they engulf foreign particulates such as bacteria or apoptotic cells. Tissue macrophages originate from hematopoietic progenitors in the embryonic yolk sac (1). However, macrophages can also be derived from hematopoietic stem cells (HSC) into myeloid precursors, which can then differentiate into monocytes and, finally, macrophages (2). Macrophages sense pathogen-associated molecular patterns (PAMP) via pattern-recognition receptors (PRR) to clear pathogens and damage-associated molecular patterns (DAMP) to activate tissue repair (3). Dysregulation of macrophage function is linked to various diseases, including diabetes, obesity, cardiovascular disease, and infection (4–6). Since macrophages react to their environment and become polarized based on the presence of exogenous stimuli, understanding the pathways that affect and are affected by this activity could be beneficial in various disease contexts.

1.1.1 Macrophage Activation and Polarization

Macrophage activation and polarization are heavily based on the stimuli present in their environment. Macrophages exist in a spectrum of polarization states *in vivo* that are difficult to mimic *in vitro*. In culture, macrophages can be activated using known stimuli to model pro- or anti-inflammatory polarization states. Pro-inflammatory macrophages, often described as M1 or classically activated, are stimulated by lipopolysaccharide (LPS) or other pro-inflammatory cytokines such as interferon-gamma (IFNɣ) (7). In contrast, anti-inflammatory macrophages, M2 or alternatively activated, are stimulated by Th2 cytokines, including interleukin (IL) 4 or IL13, to participate in tissue remodelling and immunomodulation (7). There is now a clear recognition that

macrophage activation *in vivo* is a spectrum rather than two opposing states characterized by distinct gene expression signatures (8). Importantly, macrophage activation and polarization can be directly influenced and directed by metabolic programming.

Master metabolic regulators AMP-activated protein kinase (AMPK) and mammalian target of rapamycin complex I (mTORC1) can direct macrophage polarization. For example, heightened AMPK activity has been implicated in the anti-inflammatory polarization states of macrophages. Previous research has shown that LPS-polarized macrophages with constitutively active AMPK have decreased secretion of pro-inflammatory mediator's tumour necrosis factor α (TNFα) and interleukin (IL) 6, indicating a reduced pro-inflammatory response (9). Conversely, LPS-polarized macrophages lacking AMPK activity via silencing of the α1 and α2 subunits have heightened secretion of pro-inflammatory mediators TNFα and IL6, indicating an increased pro-inflammatory response. Additionally, abolishing AMPK activity through knockout (KO) of the β1 subunit in macrophages polarized with palmitate results in increased transcription of pro-inflammatory genes, *Tnfα, Il6, and Il1β* indicating lack of AMPK activity promotes a pro-inflammatory macrophage response (10). The role mTORC1 plays in macrophage polarization is less clear than that of AMPK. LPS-polarized macrophages with heightened levels of mTORC1 activity via TSC1 knockout have been shown to have a pronounced pro-inflammatory signature as shown by transcribed and translated levels of TNFα and IL6 (11). Additionally, IL4-polarized macrophages with higher levels of mTORC1 via TSC1 KO have a significantly impaired anti-inflammatory macrophage response shown by lack of Arginase activity and through transcription of genes such as *arginase 1* (*Arg1)* and *resistin-like α* (*Fizz1)*. However, another study found LPS-polarized macrophages lacking mTORC1 activity via deletion of mTOR or Raptor have increased transcription of *Tnfα, Il6, and Il1β* and subsequent secretion of these genes, indicating a heightened

pro-inflammatory response (12). Both AMPK and mTORC1 have a clear role in influencing macrophage response to various inflammatory stimuli. Given the influence that key metabolic regulators have on macrophage polarization, metabolic rewiring must be integral to this process.

1.1.2 Macrophage metabolism

Macrophages alter their metabolism to fit cellular needs. When macrophages are activated via pro-inflammatory signals, the pentose phosphate pathway (PPP) and glycolysis are activated to provide a burst of energy needed for inflammatory cellular function (13,14). As a result of increased pyruvate, the tricarboxylic acid (TCA) cycle accumulates by-products, leading to breaks in the cycle (15,16). Specifically, citrate and succinate accumulate in the TCA cycle and are used in other cellular programs to promote inflammation. Excess citrate feeds into paths associated with fatty acid synthesis, nitric oxide (NO) production and itaconate synthesis (17). Itaconate, a crucial metabolite directly associated with antimicrobial activity, is key to executing pro-inflammatory macrophage function. Furthermore, the accumulation of succinate stabilizes hypoxia-inducible factor (HIF)-1α, which drives the expression of inflammatory cytokines needed in the pro-inflammatory response (17–19). Pro-inflammatory macrophages utilize glutamine metabolism and arginine synthesis to produce NO, which is key in antimicrobial responses. In contrast, macrophage responses to anti-inflammatory stimuli, such as Th2 cytokines, typically shift toward sustainable energy sources, such as oxidative phosphorylation and fatty acid oxidation (20,21). Additionally, anti-inflammatory macrophages have increased flux through the arginase pathway to help promote wound healing functions (22). Understanding the metabolic signalling associated with both pro- and anti-inflammatory could help target dysregulated polarization and chronic inflammation. Therefore, investigating metabolic regulators could be beneficial in understanding how metabolism impacts inflammatory activation.

1.2 AMPK

AMPK is an evolutionarily conserved heterotrimeric serine/threonine kinase involved in regulating metabolism to maintain energetic homeostasis. Specifically, AMPK is comprised of three subunits, α, β, and ɣ, for which there are multiple genes and even more splice variants that show tissue-specific patterns of expression (23). As a master regulator of cellular metabolism, AMPK senses when AMP/ATP ratios are high, meaning cellular energy levels are low, and becomes activated to turn off energy-consuming anabolic pathways and switch on energy-producing catabolic pathways (24).

AMPK activation occurs when AMP or ADP binds to the ɣ regulatory subunit, causing a conformational change that allows for phosphorylation at threonine 172 in the activation loop by upstream kinases liver kinase B1 (LKB1), Ca^{2+}/Calmodulin-dependent protein kinase kinase β (CaMKKβ) or transforming growth factor-β (TGF-β)-activated kinase 1 (TAK1)) (25,26).

1.2.1 AMPK Function

Upon activation, AMPK phosphorylates over 100 downstream targets, impacting many branches of cellular metabolism. AMPK has a well-defined role in regulating fatty acid and cholesterol synthesis through the phosphorylation of acetyl-CoA carboxylase (ACC) and 3-hydroxy-3-methyl-glutaryl-coenzyme A reductase (HMGCR) (27,28). Additionally, AMPK inhibits protein synthesis through inactivation of mTORC1 via phosphorylation of the regulatory associated protein of TOR (Raptor) and upstream regulator tuberous sclerosis complex 2 (TSC2) (29,30). Inhibition of mTORC1 restricts its ability to activate signalling cascades associated with energy consumption. Furthermore, AMPK also promotes autophagy, a degradative mechanism used to generate energy, by conserving autophagy machinery, which allows autophagy to proceed after the energetic stress subsides (31).

1.2.2 AMPK in Health and Disease

AMPK, as an energy and nutrient-sensing kinase, is affected by the accumulation of excess nutrient levels. Overnutrition associated with metabolic disorders including, obesity, type II diabetes, atherosclerosis, and fatty liver disease, leads to dysregulated AMPK activity (10,24,32). Research shows that immune cells exhibit increased pro-inflammatory function with a lack of AMPK activity (10). Free fatty acids or bacterial endotoxins such as LPS inhibit upstream kinase LKB1, preventing AMPK activation. Conversely, increased AMPK activity is associated with anti-inflammatory immune cell function and is linked to caloric restriction and exercise, which stimulate fatty acid oxidation, energy expenditure, and preserve mitochondrial homeostasis, making AMPK an attractive therapeutic target for metabolic and inflammatory diseases (33,34).

1.3 mTORC1

The serine/threonine kinase, mTOR, plays a vital role in cell growth and metabolism and can exist as two complexes, mTORC1 or mTORC2. mTORC1 promotes cell growth and metabolism, while mTORC2 regulates cell growth and survival (35). mTORC1 consists of mTOR, Raptor, G protein β subunit-like protein (GβL) / mammalian lethal with SEC13 protein 8 (mLST8), DEP-domain-containing mTOR-interacting protein (Deptor), and the 40 kDa proline-rich Akt substrate (PRAS40) (36). In contrast, mTORC2, regulated by a rapamycin-insensitive companion of mammalian target of rapamycin (Rictor), is made up of GβL/mLST8, proline-rich protein 5 (PRR5), Deptor, and mammalian stress-activated protein kinase-interacting protein (mSIN1) (36–39).

Under conditions of energy and nutrient surplus, mTORC1 is activated by a signalling cascade involving the activation of Phosphoinositide 3-kinases (PI3K) and Akt, which inhibit

mTORC1 regulators, TSC2 and AMPK (40). Additionally, amino acids also activate mTORC1 via Rag GTPases, recruiting mTORC1 to the lysosome for activation (41).

1.3.1 mTORC1 Function

mTORC1 controls anabolic pathways and cell growth by activating targets involved in protein, lipid and nucleic synthesis and inhibition of autophagy. Key targets include eukaryotic translation initiation factor 4E binding protein 1 (4EBP1), ribosomal protein S6 kinase beta-1 (S6K), and Unc-like kinase (ULK1) (42–44). 4EBP1 and S6K are directly involved in protein synthesis. In its non-phosphorylated form, 4EBP1 inhibits protein synthesis by binding to the eukaryotic translation initiation factor 4F (eIF4F) complex. When active, mTORC1 phosphorylates 4EBP1 to cause its dissociation from the eIF4F complex, allowing it to participate in translation initiation (42). The phosphorylation of S6K is responsible for promoting mRNA translation through phosphorylation of ribosomal protein S6 (43). When mTORC1 phosphorylates ULK1, the autophagy-related protein is prevented from interacting with AMPK and facilitating autophagy (44). mTORC1 also inhibits AMPK via phosphorylation of the $\alpha 1$ and $\alpha 2$ subunits to prevent catabolic metabolism (45).

1.3.2 mTORC1 in Health and Disease

mTORC1 is vital for cellular homeostasis, promoting cell growth and producing necessary macromolecules. However, constitutive activation leads to lipid accumulation and adiposity, linked to metabolic disorders like obesity and type II diabetes (46,47). Dysregulated mTORC1 activity is also implicated in various cancers and chronic inflammatory diseases involving macrophage dysfunction, such as sarcoidosis and atherosclerosis (48–50). Chronic mTORC1 activation also impairs vital catabolic pathways by directly regulating AMPK. (45). The

dysregulation of cellular homeostasis underpinning many diseases hinges on the balance between activation and inhibition of AMPK and mTORC1.

1.4 The interplay between AMPK and mTORC1

The communication between AMPK and mTORC1 is integral to resource conservation. Under conditions of nutrient starvation, AMPK becomes activated and phosphorylates multiple targets to inhibit mTORC1 activity. One known regulation point is through phosphorylation of TSC2 at S1387 and T1227, which acts as a GTPase activating protein to rheb, facilitating the hydrolysis of GTP to inactivate mTORC1 complex (29). Additionally, AMPK can directly phosphorylate Raptor at S722 and S792 to inhibit the activity of mTORC1 via 14-3-3 binding motif inhibition (30). The last known point AMPK uses to inhibit mTORC1 activity is through phosphorylation of WDR24 in the Gator complex at S155 (51). AMPK becomes activated by glucose deprivation and then phosphorylates WDR24, which destabilizes the GATOR complex, which is integral for mTORC1 activation. Conversely, under conditions of nutrient excess, mTORC1 becomes active and can phosphorylate AMPK at the α1 subunit at Ser347 and the α2 subunit at Ser345, suppressing AMPK activity and promoting anabolic metabolism (45). Both AMPK and mTORC1 have many roles in regulating cellular homeostasis. The various cellular functions regulated by these kinases make them crucial for various cellular functions, particularly immune cell regulation.

1.5 Rationale

Metabolism is crucial for macrophage responses. Master regulators of metabolic programs such as mTORC1 and AMPK have been shown to have, although sometimes conflicting, roles in regulating macrophage polarization. Models of mTORC1 overactivity via TSC1 KO show increased pro-inflammatory macrophage signatures as shown by transcribed and translated levels

of TNFα and IL6. Furthermore, these same macrophages polarized using anti-inflammatory stimuli have a diminished response, as shown by enzymatic activity and lack of transcription of key markers of anti-inflammatory activity, including *Arg1* and *Fizz1*. Conversely, LPS-polarized macrophages lacking mTORC1 activity due to mTOR or Raptor KO have increased transcription of *Tnfα, Il6, and Il1β* and subsequent secretion of these genes, indicating a heightened pro-inflammatory response (12). The conflicting data from these papers complicates the AMPK/mTORC1 signalling axis's role in macrophage activation and polarization. Although each of these studies cuts off a signalling node through which AMPK employs mTORC1 regulation, it is difficult to discern if the effects seen are due to the activity of mTORC1 or the knocked-out proteins. To better understand how the signalling between these two integral proteins may impact macrophage function, a unique mouse model where the phosphorylation sites presumed to be responsible for AMPK-mediated mTORC1 regulation, serine 1387 on TSC2 and serine 722/792 on Raptor have been mutated to alanine (double knock-in mice; DKI) was used, thereby removing metabolic control on this crucial anabolic pathway. Using a subtle model in which single amino acids are changed to remove communication between kinases allows for the investigation of this specific signalling axes in macrophage function and provides a level of clarity not afforded by traditional models where a whole protein is knocked out.

1.6 Hypothesis and Objectives

Metabolic regulation of mTORC1 conferred by AMPK is critical for macrophage metabolism and polarization. Removing this regulatory control, macrophages will be skewed toward a more pro-inflammatory phenotype due to altered metabolic programming. To test this hypothesis, the first objective will be to characterize the Raptor/TSC2 knock-in model by measuring activity downstream of mTORC1. Next, macrophage metabolism will be assessed by

measuring autophagy initiation, protein translation, oxygen consumption, extracellular acidification, lactate secretion, and citrate synthase activity. Finally, macrophage polarization will be interrogated by measuring the transcription of known inflammatory genes, secretion of inflammatory mediators, and enzymatic activity associated with macrophage polarization states.

Chapter 2: Materials and Methods

2.1 Animals

Raptor $^{S722A;\ S792A}$ mice were generated as previously described (52). Briefly, *Raptor* $^{S722A;\ S792A}$ were generated in utero using CRISPR/Cas9 with gRNA and donor dsDNA on a C57BL/J6 background. *TSC*^{S1387A} were generated in utero using CRISPR/Cas9 with gRNA and donor dsDNA on a C57BL/J6 background. *Raptor* $^{S722A;\ S792A}$ were then crossed with *TSC2*^{S1387A} to generate WT and DKI mice (*Raptor* $^{S722A;\ S792A}$*; TSC2*^{S1387A}*).* Mice were maintained on a 12-h light/dark cycle (lights on at 7:00 a.m.) and housed at 23°C with bedding enrichment. Male and female mice ages 8–30 weeks were used to generate primary macrophages, as described below. The University of Ottawa Animal Care Committee approved all animal procedures.

2.2 Primary cell isolation and culture

Bone marrow-derived macrophages (BMDM) were isolated and cultured as previously described (10,53). Briefly, bone marrow cells were obtained from the femur and tibia by centrifugation (54). Cells were differentiated into macrophages using 20% L929-conditioned media in complete DMEM (Wisent) containing 10% FBS (Wisent) and 1% penicillin/streptomycin. Bone marrow cells were plated into 15 cm dishes and allowed to differentiate for 6–8 days. Cells were lifted by gentle scraping in 10 mM EDTA in PBS, counted, and seeded into culture plates for experiments (7.5×10^4 for 96-well plates, 5.5×10^5 for 12-well plates, and 1.5×10^6 for 6-well plates). Macrophages were polarized with 20 ng/mL recombinant IL4 (Peprotech) or 100 ng/mL LPS (*E. coli*: B4, Sigma-Aldrich).

2.3 Western Blot

BMDM were washed once with PBS and lysed using cell signaling technology lysis buffer (20 mM Tris-HCl (pH 7.5), 150 mM NaCl, 1% Triton X-100, 50 mM NaF, 1 mM EGTA, 1 mM EDTA, 2.5 mM pyrophosphate, 2 mM bis(glycerophospho)glycerol, 1 mM sodium orthovanadate). Protein concentration was determined using the bicinchoninic acid assay (BCA), and samples were equalized. Denaturing loading dye was added to the sample and then boiled for 5 min at 95°C. Samples were loaded into a 10% or 12% SDS-PAGE gel and ran at 110V until adequate separation was achieved. Gel was then transferred onto a methanol-activated polyvinylidene difluoride (PVDF) membrane using the Trans-Blot® Turbo™ Transfer System and Buffer (Bio-Rad) for 20 minutes at 25V. Following the transfer, the membrane was incubated in 5% bovine serum albumin (BSA) in TBST (20 mM Tris, 150 mM NaCl, 0.05% Tween® 20) for 1 hour at room temperature. The membrane was cut at appropriate locations and the section was placed with primary antibodies (Table 1) at 4°C overnight. Antibodies were diluted 1:1000 in 5% BSA. The next day, membranes were washed four times in TBST. Membranes were placed in a secondary Anti-rabbit IgG HRP-linked Antibody (Cell Signalling Technology 7074S) for one hour at room temperature. After the secondary antibody incubation, membranes were washed four times in TBST. Membranes were activated with Clarity™ Western ECL solution (BioRad), and protein bands were visualized with LAS 4010 ImageQuant Imaging System (General Electric) or ChemiDoc™ MP Imaging System (BIO-RAD). Band contrast was adjusted using ImageJ software.

Table 1. List of Primary Antibodies.

Target	Manufacturer
beta-Actin (13E5) Rabbit mAb HRP Conjugate	Cell Signalling Technology #5125S
phospho-S6 Ribosomal Protein (Ser235/236) (91B2) Rabbit mAb	Cell Signalling Technology #4857
S6 Ribosomal Protein (5G10) Rabbit mAb	Cell Signalling Technology #2217
Phospho-p70 S6 Kinase (Thr389) (108D2) Rabbit mAb	Cell Signalling Technology #9234
p70 S6 Kinase (49D7) Rabbit mAb	Cell Signalling Technology #2708
Phospho-4E-BP1 (Thr37/46) (236B4) Rabbit mAb	Cell Signalling Technology #2855
4E-BP1 (53H11) Rabbit mAb	Cell Signalling Technology #9644
Phospho-Acetyl-CoA Carboxylase (Ser79) (D7D11) Rabbit mAb	Cell Signalling Technology #11818
Acetyl-CoA Carboxylase (C83B10) Rabbit mAb	Cell Signalling Technology #3676
Phospho-Tuberin/TSC2 (Ser1387) (D2R3A) Rabbit mAb	Cell Signalling Technology #23402
Tuberin/TSC2 (D93F12) XP® Rabbit mAb	Cell Signalling Technology #4308
Phospho-Raptor (Ser792) (E4V6C) Rabbit mAb	Cell Signalling Technology #89146
Raptor (24C12) Rabbit mAb Antibody	Cell Signalling Technology #2280
Phospho-ULK1 (Ser555) (D1H4) Rabbit mAb	Cell Signalling Technology #5869
Phospho-ULK1 (Ser757) (D7O6U) Rabbit mAb	Cell Signalling Technology #14202
ULK1 (D8H5) Rabbit mAb	Cell Signalling Technology #8054
LC3B (D11) XP Rabbit mAb	Cell Signalling Technology #3868
SQSTM1/p62 (D1Q5S) Rabbit mAb	Cell Signalling Technology #39749
Phospho-Atg14 (Ser29) (D4B8M) Rabbit mAb	Cell Signalling Technology #92340
Atg14 (D1A1N) Rabbit mAb	Cell Signalling Technology #96752

2.4 Click Chemistry

Following treatments, BMDM were labelled using 20 μM O-propargyl puromycin for 30 minutes to label newly translated peptides. Cells were then washed once with PBS and lysed using denaturing lysis buffer (50 mM Tris-HCl (pH 7.5), 150 mM NaCl, 1 mM EDTA, 0.5% IGEPAL CA-630, 0.5% triton X-100, 100 μM sodium orthovanadate, and protease inhibitor cocktail (EDTA free)). Protein concentration was determined using the bicinchoninic acid assay (BCA), and samples were equalized. Click chemistry was performed as previously described (55), the protein samples were incubated in a buffer containing 1 mM $CuSO_4$, 2 mM THPTA, 10 mM sodium ascorbate, and 2 μM Alexa fluor 647 azide, for 30 minutes. The clicked protein lysate was then precipitated using a methanol chloroform extraction to remove excess dye from the samples. Samples were resuspended in 0.5 M EDTA and 30% SDS in PBS. Once samples were in solution, SDS was diluted to 3% using PBS. Denaturing loading dye was then added. Samples were separated using a 10% SDS-PAGE gel with trichloro ethanol (TCE) as a loading control and ran at 110V until adequate separation was achieved. Gels were imaged using a Chemi Doc MP Imaging System (BioRad) using the 594 nm laser.

2.5 Extracellular Flux Assays

Cells were seeded at 75,000 cells/well and cultured in XFe96/XF Pro Cell Culture Microplates (Agilent). Extracellular flux analysis was performed using an adapted MitoStress Test Kit (Agilent). Cartridge ports were loaded with 10x concentrations of drugs: 15 μM oligomycin, 140 μM BAM15 (Cayman Chemicals), and 10 μM rotenone/10 μM antimycin A/20 μM Hoechst 33342 (56). Data were normalized by cell counts obtained by nuclear Hoechst 33342 quantification on an EVOS FL Auto 2 (ThermoFisher) microscope and Qupath (University of Edinburgh). Bioenergetics were calculated using a worksheet template.

2.6 Citrate Synthase Assay

BMDM were washed once with PBS and lysed using RIPA lysis buffer (25 mM Tris-HCl, 150 mM NaCl, 1% NP-40, 0.1% SDS, 5 mM EDTA, 1% sodium deoxycholate, protease inhibitor cocktail tablet). An aliquot of protein lysate was taken to determine the concentration to use for normalizing. 20 µL of the sample was incubated with 200 µL of 0.1 mM Acetyl CoA, 0.2 mM 5,5'-Disthiobis(2-bitrobenzoic acid) (TNB), and 5 mM oxaloacetate. Sample absorbances were read every 15 seconds for 10 minutes at 412 nm using a BioTek Gen5 plate reader (Agilent). The following equation was used to determine enzymatic activity from absorbance reading.

$$U = \left(\frac{\Delta Absorbance\ in\ OD}{Pathlength * Extinction\ Coefficient * Stiochiometry\ of\ TNB}\right) * \left(\frac{Volume\ of\ reaction\ (\mu L)}{Volume\ of\ sample\ (\mu L) * Protein\ concentration\ (mg)}\right)$$

2.7 Lactate Assay

BMDM supernatants were collected to determine lactate concentration as previously described (57). To deproteinize samples, 15 µL of supernatant and 15 µL of 12% perchloric acid were combined, incubated for 15 minutes at 4°C, and then spun at 12,000 x g for 12 minutes at 4°C, pelleting protein and cell debris. 5 µL deproteinized supernatant was transferred to a 96-well plate. Standards were added to the 96-well plate using 0.1 - 15 mM L-lactate in 50 mM potassium phosphate. 150 µL of master mix (pH 9) containing 0.4 M hydrazine hydrate, 0.5 M glycine, and 6 mM β-NAD^+ (Sigma) was added to each well. An initial absorbance was measured at 340 nm using a BioTek Gen5 plate reader. Next, each well received 50 µL of start mix (pH 9) containing 0.4 M hydrazine hydrate, 0.5 M glycine, and 5 mg/mL lactate dehydrogenase (Sigma). The reaction was mixed for 20 minutes, and a final absorbance was obtained. The OD of each sample was corrected to the OD of the blank, and lactate levels were calculated according to the standard curve.

2.8 Transcript Expression

Total RNA was isolated from BMDM using the TriPure reagent protocol (Roche Life Sciences). Isolated RNA was resuspended in RNase/DNase-free water (Wisent) and equalized using BioTek Gen5 plate reader RNA quantification setting. An all-in-one RT kit (ABM) was used to synthesize cDNA using T100 Thermal Cycler (BioRad). To determine transcript expression, the QuantiNova™ Probe PCR kit (Qiagen) was used in combination with BlastTaq™ 2X qPCR MasterMix (ABM) with custom-designed primers (ThermoFisher). Comparative qPCR reactions were run on the Roto-Gene Q (Qiagen).

2.9 Enzyme-Linked Immunosorbant Assay (ELISA)

Cell supernatants were analyzed for TNFα, IL6, and IL10 cytokines using DuoSet® ELISA Development Systems (R&D Systems). Briefly, 96-well plates were coated with 50 µL of capture antibody overnight at room temperature. Plates were washed four times with 0.05% Tween in PBS. 150 µL of 1% BSA in PBS was added to each well and incubated for one hour at room temperature. Plates were washed again, and 50 µL of standards (15.6 – 1000 pg/mL for IL6 or 31.25 – 2000 pg/mL for TNFα and IL10) or samples, diluted in 1% BSA in PBS were added to each well and left to incubate for two hours at room temperature. Plates were washed again, and 50 µL of detection antibody, diluted in 1% BSA in PBS, was added to each well and left to incubate at room temperature for two hours. Plates were washed, and 50 µL of streptavidin-horseradish peroxidase was added for 30 minutes. Again, plates were washed, and 50 µL of substrate solution was added to each well for 20 minutes. To stop the colour reaction, 50 µL of 2N H_2SO_4 was added to each well, and the OD was measured at 540 nm using BioTek Gen5 plate reader. The OD of each sample was corrected to the OD of the blank, and cytokine levels were calculated according to the standard curve.

2.10 Arginase Activity Assay

Arginase activity in BMDM was determined as previously described (57,58). Briefly, cells were washed once with PBS and lysed using 100 µL of 0.1% Triton X-100 and 25 mM Tris-HCl (pH 7.5) supplemented with a protease inhibitor cocktail. 10 µL of samples and urea standard ranging from 0.5 - 50 µg/µL were incubated with 3.5 µL of $MnCl_2$ for 10 minutes at 56°C using T100 Thermal Cycler (BioRad) to activate arginase. Next, 10 µL of 0.5 M L-arginine (pH 9.7) was added to the reaction; samples were placed back in the T100 Thermal Cycler (BioRad) for 60 minutes at 37°C. The reaction was stopped using 90 µL of stop solution containing 35% H_2SO_4/ 27% H_3PO_4/ 38% H_2O, and 4 µL of 9% α-Isonitrosopropiophenone was added and the reaction was incubated for 30 minutes at 95°C. Reactions were removed from the T100 Thermal Cycler (BioRad) and transferred to a 96-well plate. OD was measured at 540 nm using a BioTek Gen5 plate reader. The OD of each sample was corrected to the OD of the blank, and arginase activity levels were calculated according to the standard curve and the following equation.

$$\boldsymbol{U = \frac{[Urea] * Volume\ of\ reaction\ (\mu L)}{Volume\ of\ sample\ (\mu L) * time\ incubated\ at\ 37°C * 1000}}$$

2.11 Griess Assay – Quantification of Nitric Oxide

Cell culture supernatants were collected to determine nitric oxide secretions from cells. 50 µL of cell supernatant or standard curve (sodium nitrite in H_2O ranging from 10 – 100 µM) was combined with 50 µL of Griess reagent (1% sulfanilamide, 2.5% phosphoric acid, 0.1% N-(1-naphthyl) ethylenediamine dihydrochloride in H2O) in a 96-well plate. OD was then measured at 540 nm using a BioTek Gen5 plate reader. The OD of each sample was corrected to the OD of the blank, and nitrite levels were calculated according to the standard curve.

2.12 Statistical Analysis

Statistical analysis was completed using GraphPad PRISM software (version 10.0, GraphPad Software Inc., La Jolla, CA, USA). The normality of data was assessed using the Shapiro-Wilk test ($\alpha = 0.05$). For normally distributed data, differences between groups with a single variable were determined using an unpaired t-test with Welch's correction. For non-normally distributed data, differences between groups with a single variable were determined using an unpaired Mann-Whitney U test. For data with two or more variables, a two-way analysis of variance (ANOVA) with Sidak's test for multiple comparisons was used. Data are presented as means ± standard error of the mean (SEM). Statistical significance was established at $P < 0.05$. Graphs are shown as mean±s.e.m.

Chapter 3: Results

3.1 Characterizing the DKI model

3.1.1. DKI model validation

Raptor $^{S722;\ S792}$, and TSC2^{S1387} are three of the known phosphorylation sites AMPK phosphorylates to regulate mTORC1 activation (29,30). To understand the importance of AMPK regulation through Raptor and TSC2, a phospho-deficient model where AMPK target sites were mutated from serine to alanine was used. Western blot analysis was performed on naïve BMDM protein lysate from WT, Raptor^{KI}, TSC2^{KI}, and DKI mice (Figure 1). The model was assessed under conditions of pharmacological AMPK activation using 10 μM MK-8722 to confirm the lack of phosphorylation at these sites, and it was established that phosphorylation of these sites was ablated (Figure 1).

In TSC2^{KI} and DKI BMDM, phosphorylation of TSC2^{S1387} was absent while total TSC2 protein expression remained constant between samples (Figure 1). Similarly, Raptor^{KI} and DKI BMDM exhibited a lack of phosphorylation of Raptor^{S792}, while total Raptor protein expression remained constant between samples (Figure 1). Therefore, the DKI model effectively eliminated three known phosphorylation sites AMPK employs to regulate mTORC1, rendering the model resistant to AMPK-mediated phosphorylation through TSC2 and Raptor.

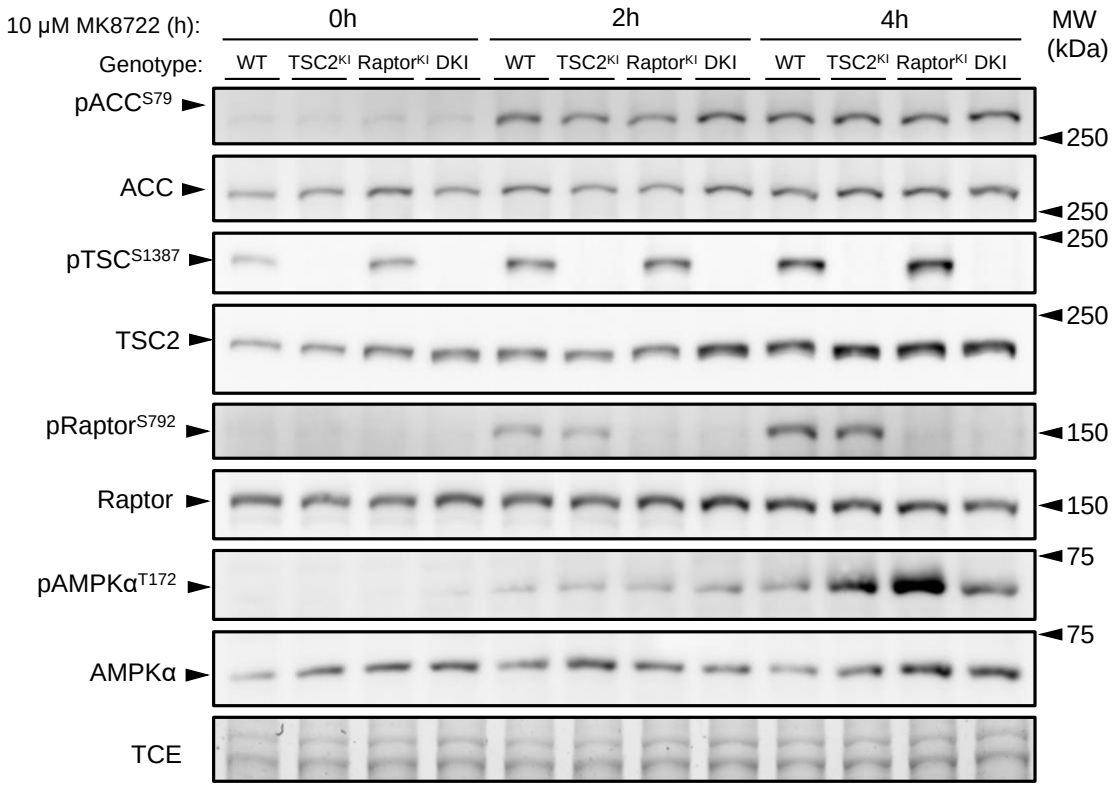

Figure 1. TSC2^{KI}, Raptor^{KI}, and DKI are resistant to AMPK-mediated phosphorylation

BMDM from WT, Raptor^{KI}, TSC2^{KI}, and DKI mice were cultured for 20 hours and then treated with 10 μM MK-8722 for 0, 2, or 4 hours prior to collection of protein lysate for western blot analysis (n=1).

3.1.2 Signalling downstream of AMPK and mTORC1

Both AMPK and mTORC1 function as serine/threonine kinases. Monitoring phosphorylation of these sites measures mTORC1 signalling, thus indicating mTORC1 activity. To measure protein signalling, western blotting was performed for targets downstream of mTORC1 involved in translation initiation, including 4EBP1$^{T37/46}$ and S6K^{T389}, which in turn phosphorylates S6$^{S245/246}$, and for targets downstream of AMPK including, ACC^{S79}, which inhibits fatty acid synthesis (Figure 2) (59,60).

Western blots were performed on protein lysate from naïve, LPS- and IL4-polarized for 24 hours BMDM from WT and DKI mice (Figure 3). BMDM were treated for one hour with 10 μM MK-8722 to activate AMPK or 250 nM Torin1 to inhibit mTOR activity. Naïve DKI BMDM exhibited unaltered mTORC1 activity as indicated by consistent phosphorylation of targets downstream, including S6K^{T389}, S6$^{S245/246}$, and 4EBP1$^{T37/46}$, in comparison to WT BMDM (Figure 3A). Furthermore, there was no consistent change in the phosphorylation of ACC^{S79}, indicating that the DKI model may not impact AMPK signalling (Figures 1 and 3A) (45).

LPS- and IL4-polarized DKI BMDM showed elevated mTORC1 activity as demonstrated by increased phosphorylation of targets downstream including S6K^{T389}, S6$^{S245/246}$, and 4EBP1$^{T37/46}$, compared to WT BMDM (Figure 3B). Additionally, ACC^{S79} phosphorylation levels remained consistent between genotypes with LPS-polarized BMDM exhibiting lower expression than IL4-polarized BMDM, likely due to higher levels of AMPK activity in IL4-polarized macrophages (61). Furthermore, LPS- and IL4-polarized WT BMDM demonstrated a decrease in phosphorylation of S6K^{T389} and S6$^{S245/246}$ when AMPK was activated pharmacologically. However, DKI BMDM showed minimal change in phosphorylation of downstream targets with AMPK activation, which indicated resistance to AMPK-mediated mTORC1 regulation.

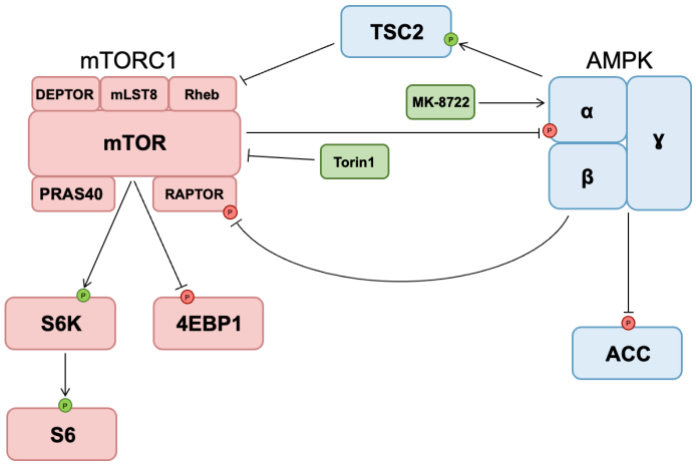

Figure 2. A schematic of phosphorylation targets downstream of AMPK and mTORC1.

Green phosphate groups are activating, and red phosphate groups are inhibiting.

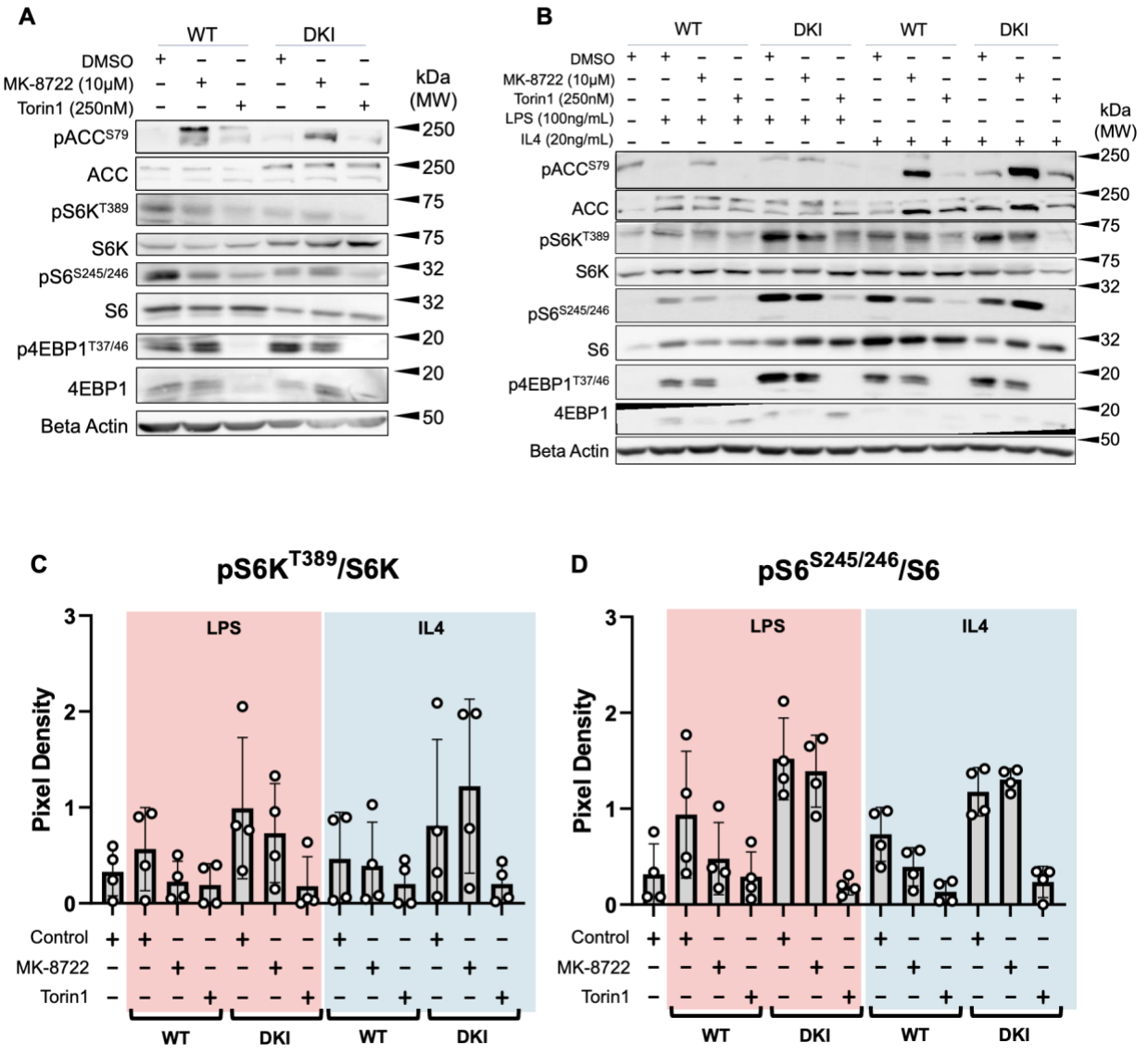

Figure 3. DKI macrophages have higher expression of targets downstream of mTORC1.

(A) BMDM were cultured for 23 hours and then treated with 10 μM MK-8722 or 250 nM Torin1 for 1 hour prior to collection of protein lysate (n=4). (B) BMDM were polarized using 100 ng/mL LPS or 20 ng/mL IL4 for 23 hours Following the polarization, cells were treated with 10 μM MK-8722 or 250 nM Torin1 for 1 hour prior to collection of protein lysate (n=4). (C, D) Pixel density of the (B) polarized blot image was determined using ImageJ for (C) S6K and (D) S6.

3.2 Metabolic characterization of WT and DKI macrophages

3.2.1 Disrupted AMPK/mTORC1 signalling does not impact autophagy initiation

Autophagy is tightly regulated by both AMPK and mTORC1 (44,62). Previous studies show that mTORC1 inhibits autophagy through phosphorylation of ULK1^{S757} in mice (Figure 4) (63). However, the notion that AMPK promotes autophagy initiation through phosphorylation of ULK^{S555} under conditions of energetic stress to maintain cellular homeostasis was recently challenged (64). Instead, it was shown that AMPK inhibits ULK1 activity to suppress autophagy initiation during conditions of energetic stress while safeguarding the ULK1-associated machinery to promote autophagy initiation when cellular homeostasis has been achieved (31).

To investigate the impact of the DKI model on autophagy initiation, western blots for autophagy initiation targets, ULK^{S757} and ATG14^{S29}, were performed on protein lysate from naïve, LPS- and IL4-polarized BMDM from WT and DKI mice (Figure 4). Autophagy initiation was impacted by conditions of AMPK activation using 10 μM MK-8722 or inhibition of mTORC1 using 250 nM Torin1 in both WT and DKI BMDM of all polarizations. Under AMPK-activated conditions, expression of ULK1^{S757} was increased and expression of ATG14^{S29} was decreased, indicating AMPK activation decreases autophagy initiation (Figure 5). The AMPK-mediated reduction in autophagy initiation matches that of previous research establishing the role AMPK plays in safeguarding autophagy machinery rather than promoting initiation (31). However, under conditions of mTORC1 inhibition, ULK1^{S757} expression decreased while ATG14^{S29} expression increased, indicating autophagy initiation increased. Increased autophagy initiation in response to lack of mTORC1 activity aligns with previous studies that established the role mTORC1 plays in autophagy inhibition (44). Furthermore, amongst both WT and DKI BMDM, ULK1^{S757} expression

matched that of total ULK1 expression after only one hour of treatment with 10 μM MK-8722 or 250 nM Torin1, indicating expression of phosphorylated ULK1 is driven by total ULK expression.

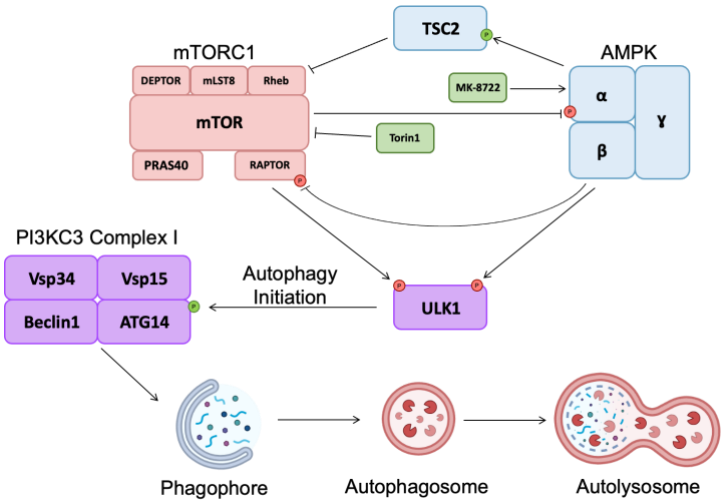

Figure 4. A schematic showing autophagy initiation downstream of AMPK and mTORC1

Green phosphate groups are activating, and red phosphate groups are inhibiting.

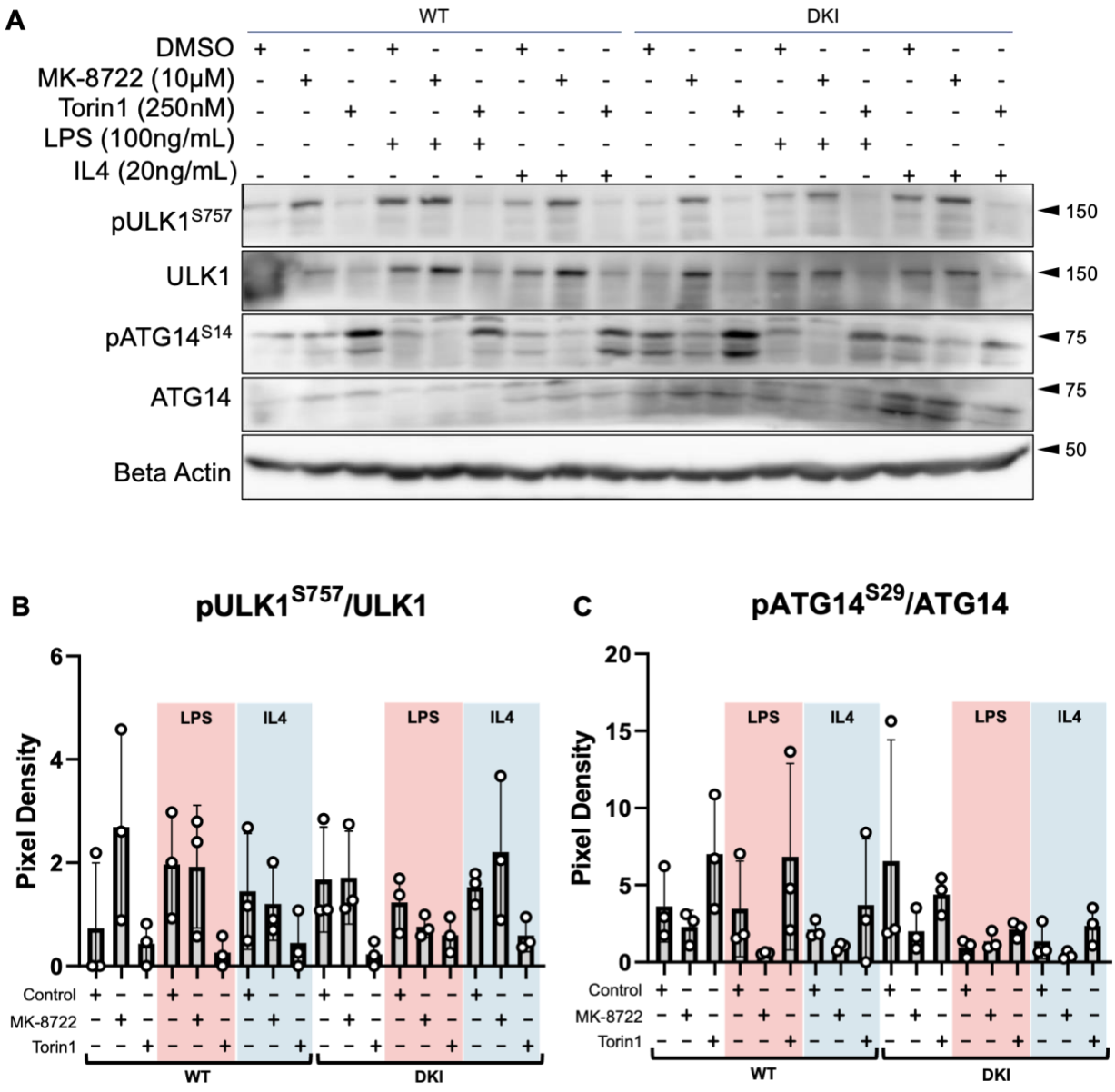

Figure 5. The Raptor/TSC2 KI mutation does not change autophagy initiation.

(A) BMDM were cultured for 23 hours either with or without 100 ng/mL LPS or 20 ng/mL IL4, then treated with 10 μM MK-8722 or 250 nM Torin1 for one hour prior to collection of protein lysate (n=3). (B, C) Pixel density of the polarized blot image was determined using ImageJ for (B) ULK1 and (C) ATG14.

3.2.2 Heightened mTORC1 activity does not affect protein translation

Under conditions of cellular homeostasis and nutrient-excess, mTORC1 is activated and facilitates the assembly of translation initiation machinery (65). Specifically, mTORC1 triggers the S6K signalling cascade, allowing S6 to contribute to translation initiation, and phosphorylates 4EBP1, which frees eIF4E to participate in the initiation of translation (42,43). Thus, in the DKI model, where mTORC1 cannot be regulated by nutrient depletion and energetic stress, translation rates should be higher even under AMPK-activated conditions.

To assess rates of protein translation, O-propargyl puromycin (OPP; a biorthogonal version of puromycin), which is a tRNA analog that can be incorporated into a growing polypeptide to inhibit protein synthesis, was added to culture to label newly synthesized peptides. Alexa Fluor 647 azide dye was linked to the OPP group using click chemistry to visualize of newly synthesized peptides. Cells were also treated with 20 μM cycloheximide (CHX), a translation inhibitor, as a negative control in the experiment. In naïve BMDM, there were no differences in rates of newly synthesized peptides between WT and DKI groups treated with MK-8722 at various times or cycloheximide (Figure 6). There were no differences in translation rates between polarizations (Figure 7). Under AMPK-activated conditions, translation rates increased in both LPS- and IL4-polarized groups in both genotypes. Additionally, BMDM treated with CHX had significantly reduced translation rates, which was expected given its role in inhibiting translation (66). Overall, DKI BMDM polarized with LPS or IL4 showed no change in global translation rates compared to WT cells (Figure 7). Hence, these results indicate that increased mTORC1 activity causes heightened expression and activation of proteins associated with translation initiation. However, this does not increase global rates of protein synthesis in BMDM.

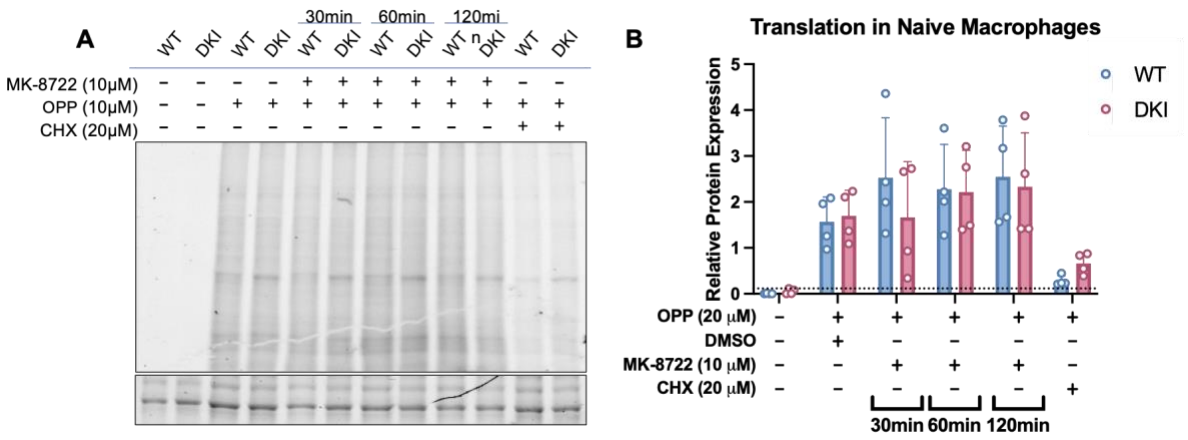

Figure 6. Disrupting AMPK-mediated mTORC1 regulation does not increase global translation in naïve BMDM.

(A) BMDM were cultured for 22.5 hours and then treated for indicated time points with 10 μM MK-8722 or treated with 20 μM cycloheximide (CHX) for 1 hour (n=4). For the last 30 minutes of cell treatments, 10 μM O-propargyl puromycin (OPP) was added to culture to label growing peptides. (B) The pixel density of the gel image was determined using ImageJ. The dotted line indicates the background as determined using the first lane of A, where no OPP was added. Graphs are shown as mean±s.e.m.

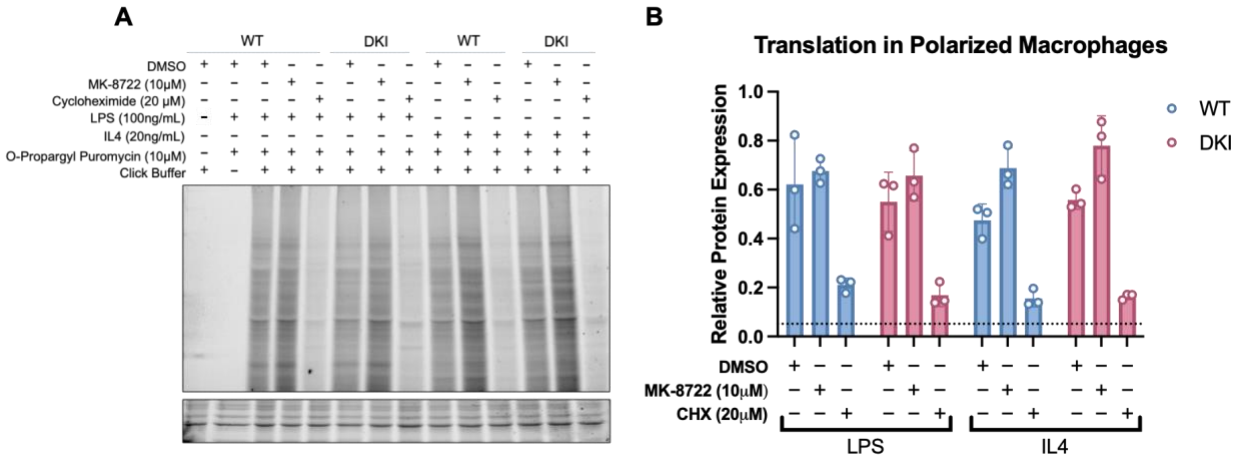

Figure 7. Disrupting AMPK-mediated mTORC1 regulation does not increase translation in polarized BMDM.

(A) BMDM were cultured for 22.5 hours 100 ng/mL LPS or 20 ng/mL IL4 for 22 hours, then treated for 1.5 hours 10 μM MK-8722 or 250 nM Torin1 (n=3). For the last 30 minutes of cell treatments, 20 μM O-propargyl puromycin was added to culture to label growing peptides. (B) The pixel density of the gel image was determined using ImageJ. The dotted line indicates the background as determined using the first lane of A, where no OPP was added. Graphs are shown as mean±s.e.m.

3.2.3 The AMPK/mTORC1 signalling axis impacts mitochondrial respiration

As master metabolic regulators, both AMPK and mTORC1 regulate metabolic homeostasis and mitochondrial function. AMPK has been shown to regulate mitochondrial biogenesis and dynamics, while mTORC1 has been implicated in regulating mitochondrial oxygen consumption and oxidative capacity (67,68). The cell mito stress test enables the assessment of mitochondrial respiration, measured by oxygen consumption rate (OCR), and glycolytic capacity, measured by extracellular acidification rate (ECAR).

In naïve and LPS-polarized BMDM, DKI cells exhibited higher OCR and ECAR compared to the WT cells (Figure 8A-D). IL4-polarized DKI BMDM showed similar rates of oxygen consumption and extracellular acidification compared to WT cells (Figure 8E-F). The observed OCR and ECAR align with the typical profiles of macrophages polarized with each stimulus. Pro-inflammatory macrophages stimulated with LPS or IFNɣ typically exhibit lower OCR compared to unstimulated or cells stimulated with anti-inflammatory Th2 cytokines such as IL4 (69,70).

Naïve and LPS-polarized DKI BMDM exhibited higher basal oxygen consumption rates, proton leak, spare respiratory capacity, and ATP production compared to the WT group (Figure 9A, B, C, D). Additionally, naïve DKI BMDM showed significantly higher rates of non-mitochondrial oxygen consumption compared to the WT BMDM (Figure 9E). LPS-polarized DKI BMDM displayed lower coupling efficiency rates compared to the WT group (Figure 9F). There were no discernible trends between the WT and DKI IL4-polarized groups. Given the increased OCR and ECAR, DKI BMDM are more metabolically active than WT cells. These cells likely utilize more oxygen to produce energy through the electron transport chain and acidifying media through increased activity through various metabolic pathways.

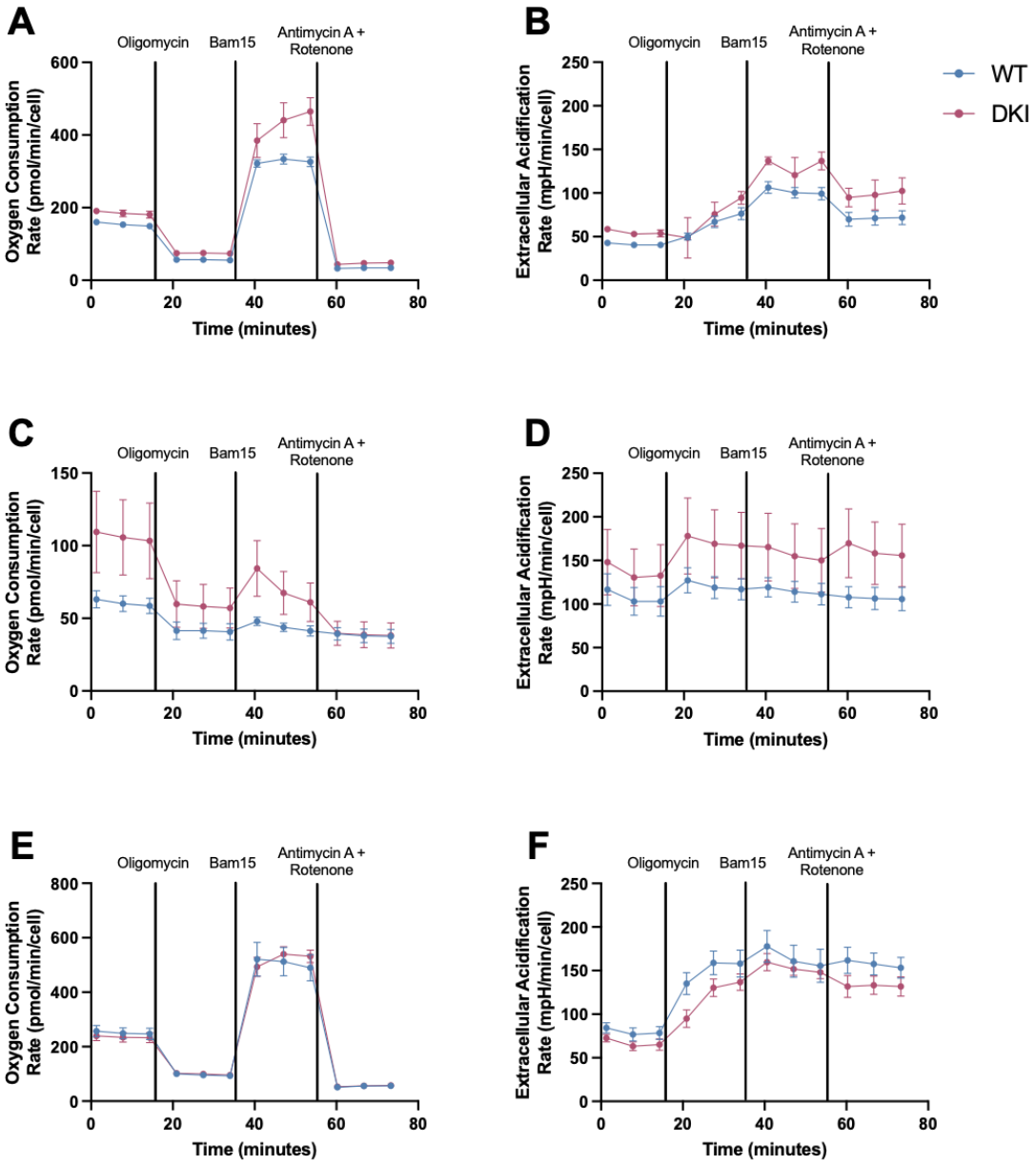

Figure 8. Increased mTORC1 activity alters mitochondrial function.

(A, C, E) Oxygen consumption rates and (B, D, F) extracellular acidification rates were measured in BMDM cultured for 24 hours with (A, B) no stimulus, (C, D) 100 ng/mL LPS, or (E, F) 20 ng/mL IL4 prior to the mito stress test using 1.5 μM Oligomycin, 14 μM Bam15, 1 μM Rotenone, and 1 μM AntimycinA (n=4). Values were normalized cell count. Graphs are shown as mean±s.e.m.

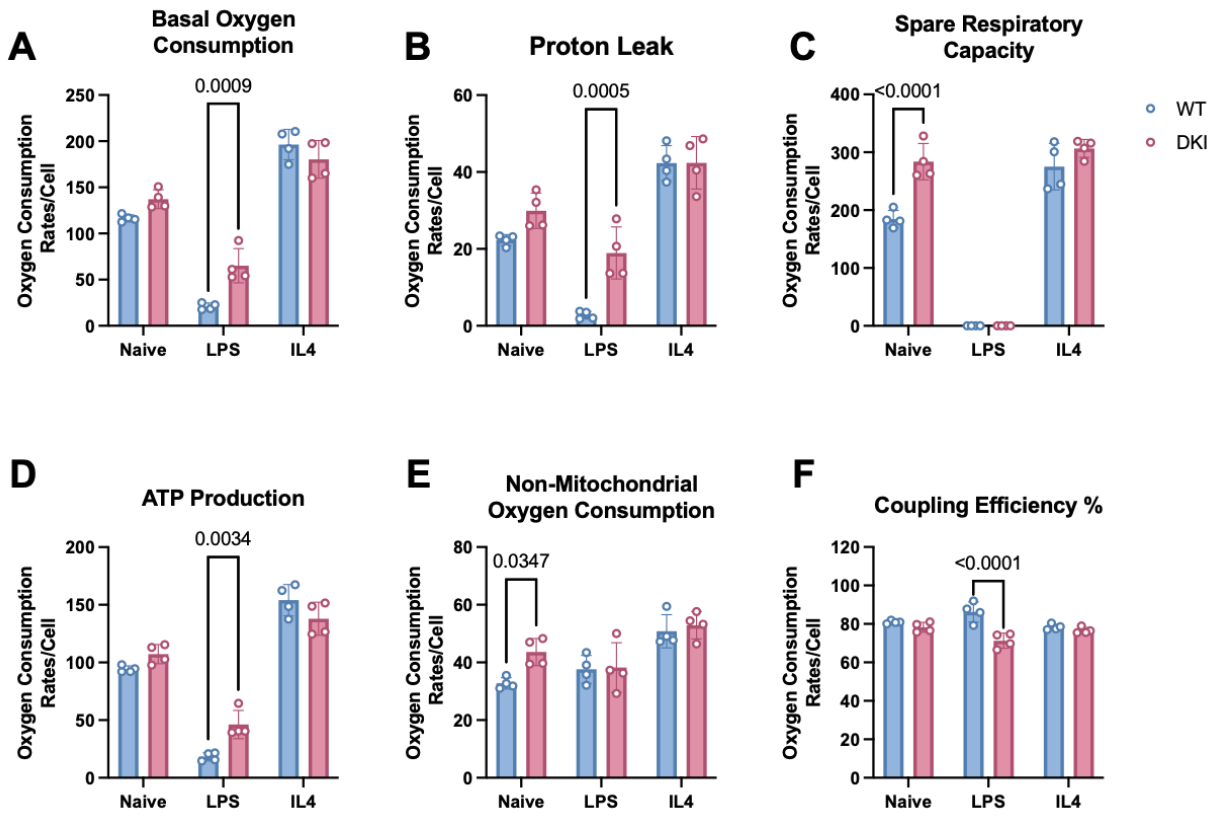

Figure 9. DKI BMDM consume more oxygen than that of WT BMDM.

(A-F) Oxygen consumption rates were measured in BMDM cultured for 24 hours with no stimulus, 100 ng/mL LPS, or 20 ng/mL IL4 prior to the mito stress test using 1.5 µM Oligomycin, 14 µM Bam15, 1 µM Rotenone, and 1 µM AntimycinA (n=4). Values were normalized cell count. Graphs are shown as mean±s.e.m. P values were determined using two-way ANOVA with Sidak's test for multiple comparisons.

3.2.4 DKI macrophages have unaltered citrate synthase activity and decreased lactate secretion

Citrate synthase is an integral enzyme to the TCA cycle and serves as a marker of mitochondrial function within the electron transport chain, making it an ideal indicator to understand changes in oxygen consumption rates (71). All polarizations showed no change in citrate synthase activity (Figure 10A). The lack of change could indicate that the DKI mutation does not impact cell metabolism through either the ETC or TCA cycle where citrate synthase activity is integral. However, further tests are needed to confirm if the AMPK/mTORC1 signalling axis influences citrate synthase activity.

Extracellular acidification can provide further information about cellular metabolism. Proton release occurs as a by-product through the hydration of CO_2 to carbonic acid from the TCA cycle and the conversion of glucose to lactate (72,73). These processes reflect distinct metabolic phenotypes, oxidative and glycolytic, respectively (74). However, the hydration of CO_2 releases three times as many protons as lactate production (73). Therefore, measuring lactate secretion is a way to investigate which phenotype the cells may be displaying. Naïve and IL4-polarized DKI BMDM showed a slight decrease in lactate secretion compared to the WT BMDM. At the same time, LPS-polarized DKI BMDM exhibited a significant decrease in lactate secretion compared to the WT cells (Figure 10B). Taken together, DKI BMDM may exhibit higher extracellular acidification rates due to increased proton production from heightened flux through the TCA cycle. Therefore, DKI BMDM may predominantly rely on the TCA cycle and oxidative phosphorylation for ATP generation. The DKI cells adopt an oxidative phenotype, demonstrated by their elevated oxygen consumption, increased extracellular acidification, and reduced lactate secretion compared to WT BMDM.

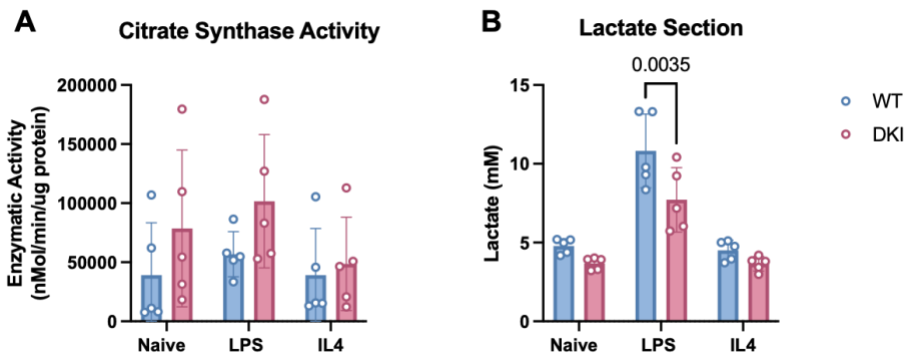

Figure 10. Lack of AMPK-mediated mTORC1 regulation does not impact citrate synthase activity and decreases lactate secretion.

(A) BMDM were cultured for 24 hours with no stimulus, 100 ng/mL LPS, or 20 ng/mL IL4 prior to collection of protein lysate to measure enzymatic activity (n=5). (B)Lactate was measured in supernatant collected from BMDM cultured for 24 hours with no stimulus, 100 ng/mL LPS, or 20 ng/mL IL4 (n=5). Graphs are shown as mean±s.e.m. P values were determined using two-way ANOVA with Sidak's test for multiple comparisons.

3.3 Assessing macrophage polarization and inflammatory activity

3.3.1 DKI macrophages have altered expression of inflammatory genes

Metabolism has long been established as a driver of macrophage activation. Both AMPK and mTORC1 influence macrophage polarization *in vitro* and *in vivo*. AMPK activity stimulates an anti-inflammatory macrophage phenotype, whereas mTORC1 promotes the pro-inflammatory phenotype (9,11). Gene expression is one of the first places where metabolism can impact inflammatory activity. Hence, transcript levels were measured to start the polarization phenotyping of this model.

DKI macrophages polarized with LPS exhibited heightened levels of pro-inflammatory transcripts, *Il6* and *Il1β*, compared to WT BMDM (Figure 11A, B). However, there were no changes in transcript levels of *Tnfα* and *Il10* between WT and DKI BMDM (Figure 11C, D). These results suggest that DKI BMDM may possess a more pro-inflammatory phenotype, consistent with previous studies investigating mTORC1 activity and macrophage polarization (11,75).

Furthermore, DKI cells polarized with IL4 had less transcript expression of *Ccl22*, which has been associated with anti-inflammatory responses, aligning with previous studies linking overactive mTORC1 with diminished anti-inflammatory macrophage responses (Figure 12A) (11). However, IL4-polarized BMDM demonstrated increased transcript expression of *Retnla*, and there was no change in *Il10* and *Arg1*, all associated with anti-inflammatory activity (Figure 12B-D). Therefore, removing AMPK-mediated mTORC1 regulation specifically affects inflammatory transcripts in response to different inflammatory stimuli.

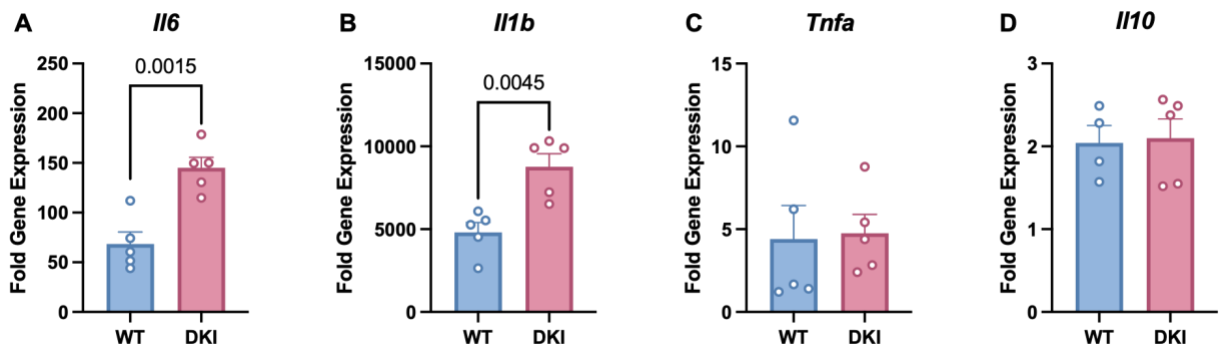

Figure 11. Heightened mTORC1 activity generally increases pro-inflammatory transcripts. BMDM were cultured for 24 hours with 100 ng/mL LPS prior to isolation of RNA (n=5). Transcript expression was normalized to the average expression of *Actb* and *Hprt* and was expressed relative to naïve WT BMDM. Graphs are shown as mean±s.e.m. P values were determined using unpaird t-test with Welch's correction.

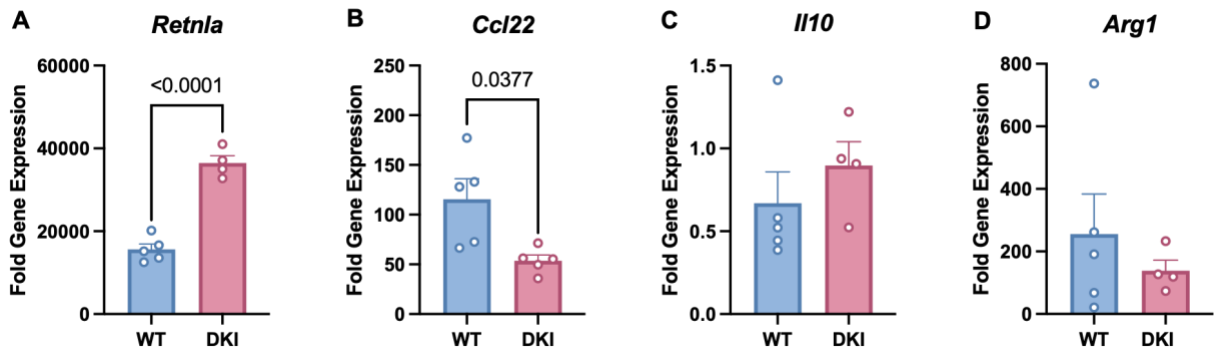

Figure 12. The Raptor/TSC2 KI mutation alters anti-inflammatory transcripts.

BMDM were cultured for 24 hours with 20 ng/mL IL4 prior to isolation of RNA (n=5). Transcript expression was normalized to the average expression of *Actb* and *Hprt* and was expressed relative to naïve WT BMDM. Graphs are shown as mean±s.e.m. P values were determined using unpaired t-test with Welch's correction.

3.3.2 Heightened mTORC1 activity decreases pro-inflammatory cytokine secretion

Upon exposure to inflammatory stimuli, macrophages undergo activation, triggering the transcription of inflammatory genes, which are subsequently translated and secreted from the cell. These cytokines serve as signalling molecules, allowing macrophages to communicate with other immune cells and coordinate a response to the inflammatory stimuli. Analyzing cytokine secretion provides valuable information about macrophage polarization and offers insight into how the surrounding environment may influence macrophage phenotype.

LPS-polarized DKI BMDM secreted significantly less TNFα and IL6 compared to the WT BMDM (Figure 13A, B). However, no change was observed in IL10 secretions between WT and DKI cells (Figure 13C). Despite unchanged *Tnfα* transcript expression between genotypes and significantly higher *Il6* transcript expression in the DKI BMDM, there was decreased cytokine secretion for both TNFα and IL6. This suggests that the DKI mutation may impact the translation of these genes, warranting further investigation. Taken together, LPS-polarized DKI BMDM exhibits reduced pro-inflammatory mediators compared to WT BMDM.

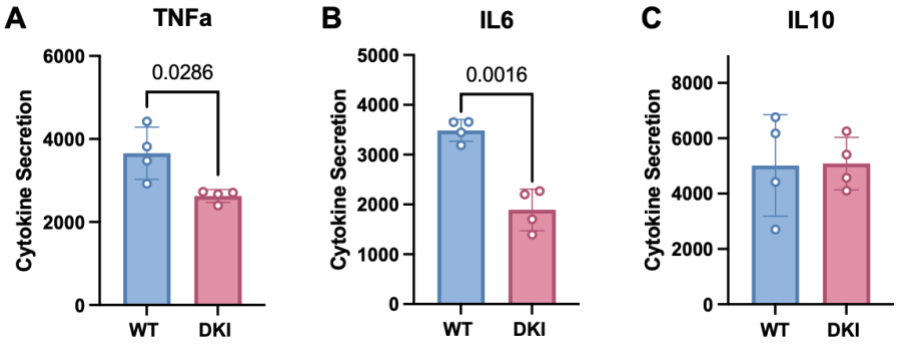

Figure 13 DKI BMDM have reduced pro-inflammatory cytokine secretions.

(A-C) Supernatant was collected from BMDM cultured for 24 hours with 100 ng/mL LPS and inflammatory cytokines were measured (n=5). Graphs are shown as mean±s.e.m. P values were determined using (A) the unpaired Mann-Whitney U test or (B-C) the unpaired t-test with Welch's correction.

3.3.3 Higher macrophage mTORC1 activity decreases arginase activity and nitrite secretion

Previous studies have demonstrated that arginase and inducible nitric oxide synthase (iNOS) work in opposition (76). Arginase serves as a marker of anti-inflammatory macrophage activity, and iNOS is a marker of pro-inflammatory activity. Arginase facilitates the hydrolysis of arginine to ornithine and urea, which are involved in promoting wound healing and anti-inflammatory activity in macrophages (77). NO, produced by iNOS from arginine and by non-enzymatic synthesis from nitrite, is involved in the infection response produced by pro-inflammatory macrophages (78,79). Additionally, research has shown that arginase can inhibit iNOS expression at the translation level, thereby inhibiting NO production (76). Investigating this signalling pathway yields valuable insights into macrophage inflammatory phenotype.

IL4-polarized DKI BMDM may have exhibited lower levels of arginase activity in comparison to WT BMDM (Figure 14A). The potential decrease in arginase activity could indicate a diminished anti-inflammatory response in macrophages. LPS-polarized DKI BMDM had no change in nitrite secretions measured in cell culture supernatant (Figure 14B). The potential decrease in arginase activity and lack of change in nitrite secretion may indicate that arginine is being converted to NO and citrulline by iNOS, consistent with previous studies investigating overactive mTORC1 and macrophage polarization (11,79). In summary, DKI macrophages exhibited a diminished anti-inflammatory response characterized by a potential decrease in arginase activity and have unchanged nitrite secretion, suggesting nitric oxide production occurs through iNOS activity, which would be a marker of pro-inflammatory macrophage activity.

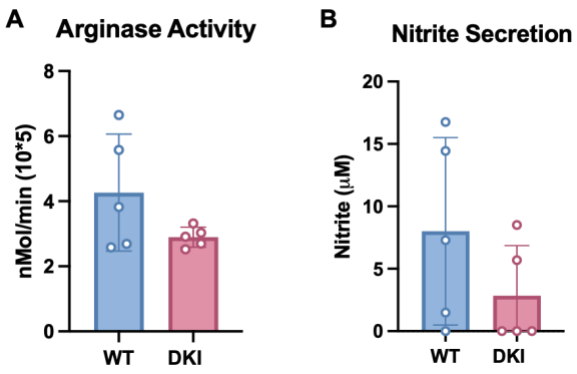

Figure 14. Lack of AMPK-mediated mTORC1 regulation decreases inflammatory responses.

(A) BMDM were cultured for 24 hours with 20 ng/mL IL4 prior to collection of protein lysate for measurement of enzymatic activity (n=5). (B) BMDM were cultured for 24 hours with 100 ng/mL LPS, and supernatant was collected to measure secretion of nitric oxide (n=5). Graphs are shown as mean±s.e.m. P values were determined using an (A) unpaired t-test with Welch's correction or an (B) unpaired Mann-Whitney U test.

Chapter 4: Discussion

4.1 Model Characterization

The intersection between the immune system and metabolism has increasingly been recognized as important in the context of immune dysfunction and metabolic diseases such as obesity, type II diabetes, and atherosclerosis. Dysregulation of the AMPK/mTORC1 has been identified as a key contributor to immune cell dysfunction (9,11,12,61,75,80–84). Early research into this signalling axis found that deletion of TSC1 leads to mTORC1 overactivity (11,84). Macrophages lacking TSC1 display enhanced pro-inflammatory and diminished anti-inflammatory functions. To delve deeper into how this signalling axis affects macrophage function, another study removed mTOR or Raptor to reduce mTORC1 activity in macrophages (12). This study revealed that reduced mTORC1 activity also increases pro-inflammatory macrophage phenotype, presenting a contradiction that complicates the understanding of mTORC1's role in macrophage function.

Previous research investigating how the AMPK/mTORC1 signalling axis may impact the innate immune system primarily involved removing entire proteins, which could inadvertently affect other pathways beyond the AMPK-mTORC1 communication (11,12,84). A precise point mutant model targeting this crucial signalling node was used to determine if the skewed polarization observed in these studies was due to a lack of AMPK-mediated mTORC1 regulation. Instead of removing proteins, which might have roles in other processes critical to macrophage polarization, this study employed a model where multiple known sites AMPK uses to inhibit mTORC1 activity were mutated from serine to alanine, preventing phosphorylation. This approach ensured that any observed results directly stem from overactive mTORC1 due to the lack of AMPK-mediated regulation.

The model in this study maintained the functionality of all proteins and kinases, ensuring that any observed outcomes were solely attributable to overactive mTORC1 due to disrupted AMPK communication. First, the absence of protein expression of the regulatory sites, Raptor$^{S722;792}$ and TSC2^{S1387} was confirmed (Figure 1). Subsequently, the activity of mTORC1 was measured by monitoring the phosphorylation of validated downstream targets, S6K^{T389}, S6$^{S245/246}$, and 4EBP1$^{T37/46}$ (Figure 3). There was a clear increase in phosphorylation downstream of mTORC1, which indicated the DKI model had increased mTORC1 activity, consistent with the findings from the TSC1 KO study (Figure 3) (11). This heightened mTORC1 activity did not impact AMPK function as measured by phosphorylation of ACC^{S79} (Figure 3). Thus, disrupting AMPK-mediated mTORC1 regulation increases mTORC1 activity and does not impact AMPK function.

4.2 Cellular Processes and Metabolic Regulation

4.2.1 Autophagy

mTORC1 is a well-established autophagy inhibitor by direct phosphorylation of ULK1, the kinase responsible for activating complexes involved in autophagy initiation. Autophagy initiation is repressed under various contexts of mTORC1 activation, such as nutrient surplus and pharmacological activation (23). Conversely, AMPK was an established autophagy activator via direct phosphorylation of ULK1. In almost all contexts, AMPK activation was synonymous with autophagy initiation (44,62). However, this notion was recently challenged, and research has shown that AMPK activation does not promote autophagy initiation (31). The role AMPK plays in autophagy initiation was reframed. Rather, Park et al. (2023) showed that AMPK is responsible for safeguarding autophagy-associated machinery to allow the process to occur after energetic stress subsides (31,63). In the Raptor/TSC2 KI model, there was no genotype effect in autophagy initiation, as indicated by the expression of proteins involved in the autophagy initiation pathway

(Figure 5). However, clear treatment effects were observed in both the WT and DKI groups. Upon AMPK activation, there was decreased phosphorylation of ATG14^{S29}, an autophagy initiation target downstream of ULK1, indicating that AMPK inhibits this signal, which aligns with the results from Park et al. (2023). Furthermore, pharmacological inhibition of mTOR using Torin1 decreased the phosphorylation of ULK1^{S757} and increased the phosphorylation of ATG14^{S29}, indicating higher rates of autophagy initiation. Overall, the treatment effects observed in this study align well with the work previously done investigating the role both AMPK and mTORC1 play in autophagy initiation (31). The work done in this study complements the reframed notion of the role AMPK plays in autophagy initiation. However, the question of whether heightened mTORC1 activity impacts autophagy remains. Future work with this model should investigate other aspects of autophagy, including lysosomal homeostasis and autophagic flux, to determine if the Raptor/TSC2 KI model impacts other aspects of the process.

4.2.2 Protein Synthesis

It is well known that mTORC1 promotes anabolic pathways, including nucleotide, lipid and protein synthesis. Often, phosphorylation of targets associated with translation initiation are used as markers of mTORC1 activity, including S6K^{T389}, S6$^{S245/246}$, and 4EBP1$^{T37/46}$ (60). However, promoting the formation of the translation initiation complex does not necessarily indicate translation rates will be higher. AMPK, the guardian of energetic homeostasis, has a well-established role in inhibiting translation, given the high amounts of energy translation consumes to carry out the process. Specifically, AMPK can prevent translation initiation by inhibiting mTORC1 through phosphorylation of Gator, Raptor, and TSC2 to prevent activation of the translation initiation complex. AMPK also inhibits translation elongation via phosphorylation of eukaryotic elongation factor 2 (eEF2^{T56}) (85). In the DKI model, some of the inhibitory signals

AMPK employs to regulate mTORC1 have been removed, meaning mTORC1 is free to promote protein synthesis. However, in this model, AMPK is active and can phosphorylate every other downstream target except those involved in regulating mTORC1. Therefore, AMPK could be phosphorylating $eEF2^{T56}$ to prevent translation elongation from occurring, which could explain the lack of genotype effect observed in this model (Figure 6, 7). Although there is no change in global translation rates between genotypes, there were clear and expected effects of macrophage polarization (Figure 7). Macrophages polarized with either LPS or IL4 had higher protein translation rates than naïve macrophages, which was an expected finding given the cellular programs activated by each stimulus (86,87). AMPK activation slightly increased translation rates in both WT and DKI cells of all polarizations. The slight increase in global translation observed upon treatment with MK-8722 could be due to AMPK shifting the cell towards translating specific proteins associated with the resolution of perceived energetic stress. This unexpected result could also be due to the off-target effects of MK-8722 (88). Upon treatment with cycloheximide to inhibit translation, translation rates decreased significantly (66). Taken together, no genotype-specific effects regarding whole-cell protein translation were observed. Future studies investigating protein translation and the AMPK/mTORC1 signalling axis should determine which transcripts are being translated to better understand how pharmacological AMPK activation impacts mRNA translation.

4.2.3 Metabolism

AMPK and mTORC1 are key regulators of metabolism, which greatly influences immune cell function. Oxidative phenotypes are associated with anti-inflammatory immune cell functions, while glycolytic phenotypes are linked to pro-inflammatory immune cell functions (86,87). Assessing OCR and ECAR through the cell mito stress test provides insights into cellular

metabolism. Increased OCR typically indicates the generation of energy through the electron transport chain, while ECAR reflects media acidification due to either hydration of CO_2 or lactate secretion, marking glycolytic activity.

Researchers investigated how lack of mTORC1 activity, achieved through genetic deletion of key mTORC1 components mTOR and Raptor, affects cell function and metabolism (12). They found that macrophages lacking mTORC1 activity exhibited lower glycolytic function measured by ECAR and decreased oxidative capacity indicated by lower OCR. Overall, macrophages lacking functional mTORC1 were less metabolically active, aligning with its role in promoting anabolic cell metabolism. Additionally, these cells had lower concentrations of TCA metabolites and lactate, suggesting an association between mTORC1 activity and increased metabolic capacity.

To understand how increased mTORC1 activity may impact cell metabolism, both ECAR and OCR were measured along with extracellular lactate levels and intracellular citrate synthase activity. IL4-polarized BMDM had no change in OCR, ECAR, extracellular lactate secretion, or citrate synthase activity (Figure 8-10). The absence of a genotype effect in IL4-polarized WT and DKI cells is anticipated due to the minimal mTORC1 activity during IL4 polarization and the well-established reliance of IL4-polarized macrophages on the ETC and fatty acid oxidation for their energy needs (11). In contrast, naïve and LPS-polarized DKI BMDM had higher rates of oxygen consumption and extracellular acidification (Figure 8A-D, 9). Additionally, these cells had decreased extracellular lactate secretion (Figure 10B). Overall, naïve and LPS-polarized macrophages with disrupted AMPK-mediated mTORC1 appear more metabolically active than their WT counterparts, which aligns with the expected role of mTORC1 in promoting anabolic metabolism.

It is well established that macrophages polarized with LPS display an energetic phenotype due to the heightened energetic demand to combat the pro-inflammatory stimulus (89). To meet these energetic demands, LPS-polarized immune cells have higher levels of mTORC1 activity. Therefore, it is not surprising that the Raptor/TSC2 KI macrophages displayed increased metabolic activity, which aligns well with the energetic metabolic phenotype. Previous studies have highlighted the effects mTORC1 has in promoting glycolysis. Specifically, mTORC1 promotes the transcription and translation of HIF-1α, Myc, Glucose transporter protein type I (GLUT1), and hexokinase 2, all of which are integral to glycolysis (90–93). mTORC1 also promotes mitochondrial metabolism through Peroxisome proliferator-activated receptor-gamma coactivator (PGC1α) and Ying Yang 1 (YY1) (94). Taken together, mTORC1 activation promotes transcription, translation, and activation of various proteins required for ATP generation through glycolysis and mitochondrial metabolism, both of which are associated with an energetic phenotype. Therefore, the energetic phenotype observed in the Raptor/TSC2 KI model is likely due to the heightened mTORC1 activity, which promotes glycolysis and mitochondrial metabolism through transcription, translation, and activation of HIF1a, Myc, GLUT1, hexokinase 2, PGC1a, and YY1. Measuring transcript and protein expression levels of the listed proteins and other known metabolic proteins should be a future step for this project to understand how heightened mTORC1 activity pushes macrophages to display an energetic metabolic phenotype.

4.5 Macrophage polarization

Metabolism is directly linked to immune cell function. Many studies have established that immune cells rely on metabolic reprogramming to differentiate and execute various functions (95). Both AMPK and mTORC1 have been shown to greatly influence metabolism and, therefore,

polarization of immune cells. Lack of AMPK activity leads to chronic pro-inflammatory polarization shown *in vitro* and is implicated in the inflammation associated with various metabolic disorders (10,32,53,96). In contrast, mTORC1 overactivity has been thought to play an important role in pro-inflammatory macrophage polarization, given its heightened activity in various diseases (11,12,50,89). However, the two studies investigating mTORC1 activity and macrophage function showed contradicting results (11,12). Overactive mTORC1 via TSC1 KO shows higher pro-inflammatory macrophage function (11). While diminished mTORC1 activity via removal of mTORC1 components, Raptor and mTOR also resulted in higher pro-inflammatory macrophage function, complicating the role that mTORC1 activity may play in macrophage function (12).

The communication and regulation between AMPK and mTORC1 maintain energetic homeostasis. Removing proteins utilized in the communication between these master metabolic regulators results in extreme changes in cellular function. In the Raptor/TSC2 KI model, there were decreased markers of pro-inflammatory polarization when macrophages were stimulated with LPS through gene expression, cytokine secretion, and nitrite secretions (Figures 11, 13, and 14). The lack of a pro-inflammatory response in the DKI model is surprising, given the increased mTORC1 activity and its known role in promoting pro-inflammatory immune cell activity (40). Furthermore, these cells likely have decreased AMPK activity due to heightened mTORC1 activity, which would likely lead to the phosphorylation of the α1 and α2 subunits, resulting in the suppression of AMPK (45). Based on the previous work done in the area, increased mTORC1 activity and decreased AMPK activity are both associated with increased pro-inflammatory macrophage responses (11). Additionally, the DKI macrophages with higher mTORC1 activity have markers of higher glycolytic activity, which is typically associated with a pro-inflammatory polarization (Figure 8-10) (89). Based on the previous work done in the field and the metabolic

phenotype observed, these macrophages were expected to have a skewed pro-inflammatory polarization (40). There was higher gene expression for some of the genes typically associated with pro-inflammatory activity, but these same genes were not being translated and subsequently secreted from the cell. Therefore, the overall response elicited by LPS may be as expected in the DKI model, but the translation and secretion of pro-inflammatory mediators may be impacted by the mutation. This would align with the unchanged translation levels in Figures 6 and 7. Future steps within this study would greatly benefit from assessing whole cell transcript and protein levels to determine where the break in the immune cell response is.

The Raptor/TSC2 KI model had no consistent change in anti-inflammatory activation in macrophages stimulated with IL4 demonstrated through gene expression, cytokine secretion, and enzyme activity (Figures 12-14). It has been well established that the anti-inflammatory immune cell response depends on heightened AMPK activity (10,32,53,96). Furthermore, increased mTORC1 activity has been shown to impair the anti-inflammatory immune cell response significantly (11,12,50,89). Along with the lack of change in anti-inflammatory markers, there was no change in metabolic profiles between WT and DKI BMDM polarized with IL4 (Figure 8–10 The unaltered anti-inflammatory response in the DKI cells and the lack of metabolic change observed in the model likely indicate that the polarization change seen in previous studies is heavily based on the metabolic rewiring associated with the loss of TSC1 through various other pathways (40). Although most of the communication sites AMPK uses to regulate mTORC1 have been removed in the Raptor/TSC2 KI model, AMPK may use other known or unknown mechanisms to inhibit mTORC1 in response to IL4. Looking at macrophage response in models where all other known sites AMPK uses to regulate mTORC1 are modified would be beneficial in the search to understand how this signalling axis impacts macrophage responses.

4.6 Limitations and Considerations

This study is subject to various limitations and considerations. The first consideration in this study was the length of treatment times. This project investigated the effects of the DKI model under acute AMPK-activated and mTORC1-inhibited conditions. Although the overarching question was answered using acute treatments, in hindsight, activating AMPK and inhibiting mTORC1 for a longer period may have better displayed the genotype effects within the model. Although effects on both AMPK activation and mTORC1 inhibition were observed with a one-hour treatment, a longer treatment time would likely be necessary to see more robust downstream effects on protein signalling. Additionally, only one concentration and time point were used for all treatments and stimulations. Looking at various time points and concentrations of AMPK activation/mTORC1 inhibition along with LPS/IL4 polarizations could have provided valuable information about the model with respect to the AMPK/mTORC1 signalling axis in macrophage polarization and activation.

Another consideration is that not all the known phosphorylation sites AMPK uses to regulate mTORC1 were modified, meaning AMPK was still able to communicate with mTORC1, albeit in a much smaller capacity. While this study has three of the five known sites knocked in, AMPK is still able to regulate mTORC1 through phosphorylation of TSC2 at T1227 and WDR24 in the Gator complex at S155 (29,51). While each of these sites plays a part in AMPK-mediated mTORC1 regulation, the extent to which these sites contribute to the overall mechanism is unknown. These remaining phosphorylation sites could be why no significant genotype effects are observed in various assays. Although it is complicated to mutate further sites in a mouse model, to understand this signalling axis fully, it would be beneficial to have all known phosphorylation

sites mutated to ensure that all known AMPK-mediated mTORC1 regulatory mechanisms have been removed.

This study used primary BMDM to test immune cell polarization in a model lacking AMPK-mediated mTORC1 regulation. BMDM are a great model to work with as they have a good yield for most cell culture experiments conducted. However, BMDM are naïve immune cells and have not been subjected to various inflammatory stimuli that tissue resident and circulating macrophages may experience *in vivo*. The use of BMDM in this study provided valuable information about how macrophages exposed to either LPS or IL4 may respond with chronic mTORC1 activity, giving a very black-and-white idea of macrophage polarization. *In vivo*, macrophages are exposed to various stimuli and exist in a broad spectrum of activation states. Characterizing the metabolic and inflammatory profiles of tissue-resident macrophages with the DKI mutation would provide a more realistic idea of how AMPK and mTORC1 influence macrophage polarization and activation *in vivo*.

The final limitation of this study is the constitutive nature of the mutations introduced within this knock-in model. The mutations preventing AMPK from inhibiting mTORC1 are consistent throughout the whole body and are present from birth, which could allow for compensatory mechanisms to develop over time. These compensatory mechanisms might obscure or alter the true impact of AMPK-mediated regulation of mTORC1 on macrophage function, explaining the lack of genotype effect in certain aspects of this study. For instance, other signalling pathways or regulatory proteins might adapt to mitigate the effects of the disrupted AMPK/mTORC1 interaction, leading to an underestimation or misinterpretation of the direct consequences of the mutations.

4.7 Future Directions

There were clear changes in the metabolic profiles of macrophages due to elevated mTORC1 activity. However, these changes were not associated with significant changes to the inflammatory response to LPS or IL4. Despite the elevated phosphorylation of proteins associated with translation initiation, heightened mTORC1 activity did not increase whole-cell protein synthesis. This finding is surprising given mTORC1's established role in upregulating protein synthesis and the increased phosphorylation of translation initiation targets. Polysome sequencing could provide valuable insights into the discrepancies between the metabolic and inflammatory phenotypes observed in the DKI model by revealing which genes are being translated. There was also a clear difference in metabolic function as seen through OCR, ECAR, and extracellular lactate levels. The next step with this project would be to investigate how increased mTORC1 activity is influencing these metabolic changes. Doing targeted metabolomics to measure levels of metabolites would show the changes within the cell and could provide insight into how AMPK-mediated mTORC1 regulation may impact macrophage polarization. Finally, there was a clear discrepancy between gene expression and cytokine secretion levels. Investigating how lack of AMPK-mediated mTORC1 regulation may impact the translation and secretion of cytokines would broaden the knowledge of the role the AMPK/mTORC1 signalling axis plays in macrophage polarization and activation. Performing RNA sequencing to measure whole-cell gene expression paired with polysome sequencing would allow for the comparison between gene and protein levels, which may be the cause of the discrepancies seen in this model.

The next step should be investigating how the DKI model impacts immune cell populations *in vivo*. In culture, there were differences in metabolism and polarization in macrophages polarized with LPS and IL4. Therefore, it would be interesting to understand if tissue and circulating

macrophages challenged in a sepsis model or a helminth infection respond similarly to the stimuli used in culture. Additionally, measuring other immune cell populations to understand how the DKI mutation may influence their activation and metabolism would be an important future step for this project. Finally, exploring how the lack of AMPK-mediated mTORC1 regulation may influence metabolic disease progression would be an interesting direction to take this project. Both AMPK and mTORC1 have a well-established role in regulating immune cell function and contributing to disease progression in various metabolic disorders, including atherosclerosis, type II diabetes, and fatty liver disease. Therefore, using the DKI model to understand how higher levels of mTORC1 may alter disease progression and severity would further the current understanding of how integral metabolic kinases are involved in these chronic disorders.

4.8 Conclusion

Both AMPK and mTORC1 are integral to cellular homeostasis. This study investigated how disrupted AMPK-mediated mTORC1 regulation impacts macrophage metabolism and polarization. This data supports the conclusion that reduced AMPK-mediated mTORC1 regulation leads to an energetic cellular phenotype in naïve and LPS-polarized macrophages. Furthermore, this data shows that increased macrophage mTORC1 reduces the inflammatory response to both LPS and IL4. The balance between AMPK and mTORC1 is crucial for maintaining cellular function. Understanding how dysregulation between these key kinases impacts immune cell function may provide further insights into better treatments for metabolic diseases where the balance between AMPK and mTORC1 is disrupted.

References

1. Palis J, Robertson S, Kennedy M, Wall C, Keller G. Development of erythroid and myeloid progenitors in the yolk sac and embryo proper of the mouse. Development [Internet]. 1999 Nov 15 [cited 2022 Nov 28];126(22):5073–84. Available from: https://journals.biologists.com/dev/article/126/22/5073/40558/Development-of-erythroid-and-myeloid-progenitors

2. Le Douce V, Herbein G, Rohr O, Schwartz C. Molecular mechanisms of HIV-1 persistence in the monocyte-macrophage lineage. Retrovirology. 2010 Apr 9;7.

3. Schenten D, Medzhitov R. The Control of Adaptive Immune Responses by the Innate Immune System. Adv Immunol. 2011;109:87–124.

4. Lavine KJ, Pinto AR, Epelman S, Kopecky BJ, Clemente-Casares X, Godwin J, et al. The Macrophage in Cardiac Homeostasis and Disease: JACC Macrophage in CVD Series. J Am Coll Cardiol [Internet]. 2018 Oct 10 [cited 2022 Nov 28];72(18):2213. Available from: /pmc/articles/PMC6209119/

5. Alrdahe S, Al Sadoun H, Torbica T, McKenzie EA, Bowling FL, Boulton AJM, et al. Dysregulation of macrophage development and phenotype in diabetic human macrophages can be rescued by Hoxa3 protein transduction. PLoS One [Internet]. 2019 Oct 1 [cited 2022 Nov 28];14(10). Available from: /pmc/articles/PMC6799902/

6. Reece MD, Taylor RR, Song C, Gavegnano C. Targeting Macrophage Dysregulation for Viral Infections: Novel Targets for Immunomodulators. Front Immunol [Internet]. 2021 Nov 1 [cited 2022 Nov 28];12. Available from: /pmc/articles/PMC8591232/

7. Mills CD, Kincaid K, Alt JM, Heilman MJ, Hill AM. M-1/M-2 Macrophages and the Th1/Th2 Paradigm. The Journal of Immunology [Internet]. 2000 Jun 15 [cited 2022 Nov 28];164(12):6166–73. Available from: https://journals.aai.org/jimmunol/article/164/12/6166/33085/M-1-M-2-Macrophages-and-the-Th1-Th2-Paradigm1

8. Murray PJ, Allen JE, Biswas SK, Fisher EA, Gilroy DW, Goerdt S, et al. Macrophage activation and polarization: nomenclature and experimental guidelines. Immunity [Internet]. 2014 Jul 7 [cited 2022 Nov 28];41(1):14. Available from: /pmc/articles/PMC4123412/

9. Sag D, Carling D, Stout RD, Suttles J. AMP-activated protein kinase promotes macrophage polarization to an anti-inflammatory functional phenotype. J Immunol [Internet]. 2008 Dec 12 [cited 2024 May 2];181(12):8633. Available from: /pmc/articles/PMC2756051/

10. Galic S, Fullerton MD, Schertzer JD, Sikkema S, Marcinko K, Walkley CR, et al. Hematopoietic AMPK β1 reduces mouse adipose tissue macrophage inflammation and insulin resistance in obesity. J Clin Invest [Internet]. 2011 Dec 1 [cited 2024 Apr 22];121(12):4903–15. Available from: https://pubmed.ncbi.nlm.nih.gov/22080866/

11. Byles V, Covarrubias AJ, Ben-Sahra I, Lamming DW, Sabatini DM, Manning BD, et al. The TSC-mTOR pathway regulates macrophage polarization. Nat Commun [Internet]. 2013 Nov 27 [cited 2024 Apr 30];4:2834. Available from: /pmc/articles/PMC3876736/

12. Collins SL, Oh MH, Sun IH, Chan-Li Y, Zhao L, Powell JD, et al. mTORC1 Signaling Regulates Proinflammatory Macrophage Function and Metabolism. The Journal of Immunology [Internet]. 2021 Aug 1 [cited 2024 May 9];207(3):913–22. Available from: https://dx.doi.org/10.4049/jimmunol.2100230

13. Haschemi A, Kosma P, Gille L, Evans CR, Burant CF, Starkl P, et al. The sedoheptulose kinase CARKL directs macrophage polarization through control of glucose metabolism. Cell Metab. 2012 Jun 6;15(6):813–26.

14. Palsson-Mcdermott EM, Curtis AM, Goel G, Lauterbach MAR, Sheedy FJ, Gleeson LE, et al. Pyruvate Kinase M2 regulates Hif-1α activity and IL-1β induction, and is a critical determinant of the Warburg Effect in LPS-activated macrophages. Cell Metab [Internet]. 2015 Jan 1 [cited 2022 Nov 28];21(1):65. Available from: /pmc/articles/PMC5198835/

15. Lauterbach MA, Hanke JE, Serefidou M, Mangan MSJ, Kolbe CC, Hess T, et al. Toll-like Receptor Signaling Rewires Macrophage Metabolism and Promotes Histone Acetylation via ATP-Citrate Lyase. Immunity. 2019 Dec 17;51(6):997-1011.e7.

16. O'Neill LAJ, Kishton RJ, Rathmell J. A guide to immunometabolism for immunologists. Nature Reviews Immunology 2016 16:9 [Internet]. 2016 Jul 11 [cited 2024 May 25];16(9):553–65. Available from: https://www.nature.com/articles/nri.2016.70

17. Meiser J, Krämer L, Sapcariu SC, Battello N, Ghelfi J, D'Herouel AF, et al. Pro-inflammatory macrophages sustain pyruvate oxidation through pyruvate dehydrogenase for the synthesis of itaconate and to enable cytokine expression. Journal of Biological Chemistry [Internet]. 2016 Feb 19 [cited 2022 Nov 28];291(8):3932–46. Available from: http://www.jbc.org/article/S0021925820437019/fulltext

18. Jha AK, Huang SCC, Sergushichev A, Lampropoulou V, Ivanova Y, Loginicheva E, et al. Network integration of parallel metabolic and transcriptional data reveals metabolic modules that regulate macrophage polarization. Immunity. 2015 Mar 17;42(3):419–30.

19. Cordes T, Wallace M, Michelucci A, Divakaruni AS, Sapcariu SC, Sousa C, et al. Immunoresponsive gene 1 and itaconate inhibit succinate dehydrogenase to modulate intracellular succinate levels. Journal of Biological Chemistry [Internet]. 2016 Jul 1 [cited 2022 Nov 28];291(27):14274–84. Available from: http://www.jbc.org/article/S0021925820367703/fulltext

20. Vats D, Mukundan L, Odegaard JI, Zhang L, Smith KL, Morel CR, et al. Oxidative metabolism and PGC-1β attenuate macrophage-mediated inflammation. Cell Metab. 2006;4(1):13–24.

21. Varga T, Mounier R, Horvath A, Cuvellier S, Dumont F, Poliska S, et al. Highly Dynamic Transcriptional Signature of Distinct Macrophage Subsets during Sterile Inflammation,

Resolution, and Tissue Repair. The Journal of Immunology [Internet]. 2016 Jun 1 [cited 2022 Nov 28];196(11):4771–82. Available from: https://journals.aai.org/jimmunol/article/196/11/4771/105136/Highly-Dynamic-Transcriptional-Signature-of

22. Albina JE, Mills CD, Barbul A, Thirkill CE, Henry WL, Mastrofrancesco B, et al. Arginine metabolism in wounds. https://doi.org/101152/ajpendo19882544E459 [Internet]. 1988 [cited 2024 May 25];254(4). Available from: https://journals.physiology.org/doi/10.1152/ajpendo.1988.254.4.E459

23. Willows R, Navaratnam N, Lima A, Read J, Carling D. Effect of different γ-subunit isoforms on the regulation of AMPK. Biochemical Journal [Internet]. 2017 May 5 [cited 2022 Dec 4];474(10):1741. Available from: /pmc/articles/PMC5423082/

24. Winder WW, Hardie DG. AMP-activated protein kinase, a metabolic master switch: Possible roles in Type 2 diabetes. Am J Physiol Endocrinol Metab. 1999;277(1 40-1).

25. Carling D, Sanders MJ, Woods A. The regulation of AMP-activated protein kinase by upstream kinases. International Journal of Obesity 2008 32:4 [Internet]. 2008 Aug 21 [cited 2022 Nov 28];32(4):S55–9. Available from: https://www.nature.com/articles/ijo2008124

26. Momcilovic M, Hong SP, Carlson M. Mammalian TAK1 activates Snf1 protein kinase in yeast and phosphorylates AMP-activated protein kinase in vitro. J Biol Chem [Internet]. 2006 Sep 1 [cited 2024 May 25];281(35):25336–43. Available from: https://pubmed.ncbi.nlm.nih.gov/16835226/

27. Carlson CA, Kim KH. Regulation of Hepatic Acetyl Coenzyme A Carboxylase by Phosphorylation and Dephosphorylation. Journal of Biological Chemistry. 1973 Jan 10;248(1):378–80.

28. Beg ZH, Allmann DW, Gibson DM. Modulation of 3-hydroxy-3-methylglutaryl coenzyme A reductase activity with cAMP and with protein fractions of rat liver cytosol. Biochem Biophys Res Commun. 1973 Oct 15;54(4):1362–9.

29. Inoki K, Zhu T, Guan KL. TSC2 Mediates Cellular Energy Response to Control Cell Growth and Survival. Cell [Internet]. 2003 Nov 26 [cited 2024 May 21];115(5):577–90. Available from: http://www.cell.com/article/S0092867403009292/fulltext

30. Gwinn DM, Shackelford DB, Egan DF, Mihaylova MM, Mery A, Vasquez DS, et al. AMPK Phosphorylation of Raptor Mediates a Metabolic Checkpoint. Mol Cell [Internet]. 2008 Apr 25 [cited 2024 May 21];30(2):214–26. Available from: http://www.cell.com/article/S109727650800169X/fulltext

31. Park JM, Lee DH, Kim DH. Redefining the role of AMPK in autophagy and the energy stress response. Nature Communications 2023 14:1 [Internet]. 2023 May 24 [cited 2024 May 7];14(1):1–17. Available from: https://www.nature.com/articles/s41467-023-38401-z

32. Day EA, Townsend LK, Rehal S, Batchuluun B, Wang D, Morrow MR, et al. Macrophage AMPK β1 activation by PF-06409577 reduces the inflammatory response, cholesterol synthesis, and atherosclerosis in mice. iScience. 2023 Nov 17;26(11):108269.

33. Weir HJ, Yao P, Huynh FK, Escoubas CC, Goncalves RL, Burkewitz K, et al. Dietary Restriction and AMPK Increase Lifespan via Mitochondrial Network and Peroxisome Remodeling. Cell Metab [Internet]. 2017 Dec 5 [cited 2024 May 25];26(6):884-896.e5. Available from: http://www.cell.com/article/S1550413117306125/fulltext

34. McArthur S, Juban G, … TGTJ of, 2020 undefined. Annexin A1 drives macrophage skewing to accelerate muscle regeneration through AMPK activation. Am Soc Clin InvestigS McArthur, G Juban, T Gobbetti, T Desgeorges, M Theret, J Gondin, JE Toller-KawahisaThe Journal of clinical investigation, 2020•Am Soc Clin Investig [Internet]. 2020 [cited 2024 May 23]; Available from: https://www.jci.org/articles/view/124635

35. Laplante M, Sabatini DM. mTOR Signaling in Growth Control and Disease. Cell [Internet]. 2012 Apr 13 [cited 2024 May 12];149(2):274–93. Available from: http://www.cell.com/article/S0092867412003510/fulltext

36. Hara K, Maruki Y, Long X, Yoshino K ichi, Oshiro N, Hidayat S, et al. Raptor, a binding partner of target of rapamycin (TOR), mediates TOR action. Cell [Internet]. 2002 Jul 26 [cited 2024 May 16];110(2):177–89. Available from: http://www.cell.com/article/S0092867402008334/fulltext

37. Pearce LR, Huang X, Boudeau J, Pawłowski R, Wullschleger S, Deak M, et al. Identification of Protor as a novel Rictor-binding component of mTOR complex-2. portlandpress.comLR Pearce, X Huang, J Boudeau, R Pawłowski, S Wullschleger, M Deak, AFM IbrahimBiochemical Journal, 2007•portlandpress.com [Internet]. 2007 [cited 2024 May 16];405:513–22. Available from: https://portlandpress.com/biochemj/article-abstract/405/3/513/42443

38. Sarbassov D, Ali S, Kim D, Guertin D, biology RLC, 2004 undefined. Rictor, a novel binding partner of mTOR, defines a rapamycin-insensitive and raptor-independent pathway that regulates the cytoskeleton. cell.comDD Sarbassov, SM Ali, DH Kim, DA Guertin, RR Latek, H Erdjument-Bromage, P TempstCurrent biology, 2004•cell.com [Internet]. [cited 2024 May 16]; Available from: https://www.cell.com/fulltext/S0960-9822(04)00471-3

39. Yang Q, Inoki K, Ikenoue T, development KGG&, 2006 undefined. Identification of Sin1 as an essential TORC2 component required for complex formation and kinase activity. genesdev.cshlp.orgQ Yang, K Inoki, T Ikenoue, KL GuanGenes & development, 2006•genesdev.cshlp.org [Internet]. 2006 [cited 2024 May 16]; Available from: https://genesdev.cshlp.org/content/20/20/2820.short

40. Inoki K, Li Y, Zhu T, Wu J, Guan KL. TSC2 is phosphorylated and inhibited by Akt and suppresses mTOR signalling. Nat Cell Biol [Internet]. 2002 Sep [cited 2024 May 25];4(9):648–57. Available from: https://pubmed.ncbi.nlm.nih.gov/12172553/

41. Inoki K, Li Y, Xu T, Guan KL. Rheb GTPase is a direct target of TSC2 GAP activity and regulates mTOR signaling. Genes Dev [Internet]. 2003 Aug 8 [cited 2024 May 7];17(15):1829. Available from: /pmc/articles/PMC196227/

42. Gingras AC, Raught B, Sonenberg N. eIF4 initiation factors: Effectors of mRNA recruitment to ribosomes and regulators of translation. Annu Rev Biochem [Internet]. 1999 Jul 1 [cited 2024 Apr 29];68(Volume 68, 1999):913–63. Available from: https://www.annualreviews.org/content/journals/10.1146/annurev.biochem.68.1.913

43. Holz MK, Ballif BA, Gygi SP, Blenis J. mTOR and S6K1 Mediate Assembly of the Translation Preinitiation Complex through Dynamic Protein Interchange and Ordered Phosphorylation Events. Cell. 2005 Nov 18;123(4):569–80.

44. Kim J, Kundu M, Viollet B, Guan KL. AMPK and mTOR regulate autophagy through direct phosphorylation of Ulk1. Nat Cell Biol [Internet]. 2011 Feb [cited 2024 Apr 29];13(2):132. Available from: /pmc/articles/PMC3987946/

45. Ling NXY, Kaczmarek A, Hoque A, Davie E, Ngoei KRW, Morrison KR, et al. mTORC1 directly inhibits AMPK to promote cell proliferation under nutrient stress. Nat Metab [Internet]. 2020 Jan 1 [cited 2024 Apr 30];2(1):41–9. Available from: https://pubmed.ncbi.nlm.nih.gov/31993556/

46. Polak P, Cybulski N, Feige JN, Auwerx J, Rü Egg MA, Hall MN. Adipose-specific knockout of raptor results in lean mice with enhanced mitochondrial respiration. cell.comP Polak, N Cybulski, JN Feige, J Auwerx, MA Rüegg, MN HallCell metabolism, 2008•cell.com [Internet]. 2008 [cited 2024 May 25]; Available from: https://www.cell.com/cell-metabolism/pdf/S1550-4131(08)00287-8.pdf

47. Dü K, Yecies JL, Menon S, Raman P, Lipovsky AI, Souza AL, et al. Activation of a metabolic gene regulatory network downstream of mTOR complex 1. cell.comK Düvel, JL Yecies, S Menon, P Raman, AI Lipovsky, AL Souza, E Triantafellow, Q MaMolecular cell, 2010•cell.com [Internet]. 2010 [cited 2024 May 25]; Available from: https://www.cell.com/molecular-cell/pdf/S1097-2765(10)00463-6.pdf

48. Zou Z, Tao T, Li H, bioscience XZC&, 2020 undefined. mTOR signaling pathway and mTOR inhibitors in cancer: progress and challenges. SpringerZ Zou, T Tao, H Li, X ZhuCell & bioscience, 2020•Springer [Internet]. 2020 Mar 10 [cited 2024 May 25];10(1). Available from: https://link.springer.com/article/10.1186/s13578-020-00396-1

49. Zhang Q, Hu J, Wu Y, Luo H, Meng W, Xiao B, et al. Rheb (Ras homolog enriched in brain 1) Deficiency in mature macrophages prevents atherosclerosis by repressing macrophage proliferation, inflammation, and lipid uptake. Arterioscler Thromb Vasc Biol [Internet]. 2019 Jan 8 [cited 2022 Dec 3];39(9):1787–801. Available from: https://www.ahajournals.org/doi/suppl/10.1161/ATVBAHA.119.312870.

50. Linke M, Pham HTT, Katholnig K, Schnöller T, Miller A, Demel F, et al. Chronic signaling via the metabolic checkpoint kinase mTORC1 induces macrophage granuloma formation

and marks sarcoidosis progression. Nature Immunology 2017 18:3 [Internet]. 2017 Jan 16 [cited 2022 Dec 3];18(3):293–302. Available from: https://www.nature.com/articles/ni.3655

51. Dai X, Jiang C, Jiang Q, Fang L, Yu H, Guo J, et al. AMPK-dependent phosphorylation of the GATOR2 component WDR24 suppresses glucose-mediated mTORC1 activation. Nature Metabolism 2023 5:2 [Internet]. 2023 Feb 2 [cited 2024 May 21];5(2):265–76. Available from: https://www.nature.com/articles/s42255-022-00732-4

52. van Nostrand JL, Hellberg K, Luo EC, van Nostrand EL, Dayn A, Yu J, et al. AMPK regulation of Raptor and TSC2 mediate metformin effects on transcriptional control of anabolism and inflammation. Genes Dev [Internet]. 2020 Oct 1 [cited 2024 Apr 29];34(19–20):1330–44. Available from: https://pubmed.ncbi.nlm.nih.gov/32912901/

53. Fullerton MD, Ford RJ, McGregor CP, LeBlond ND, Snider SA, Stypa SA, et al. Salicylate improves macrophage cholesterol homeostasis via activation of Ampk. J Lipid Res [Internet]. 2015 May 1 [cited 2024 Apr 22];56(5):1025–33. Available from: http://www.jlr.org/article/S0022227520312426/fulltext

54. Snider SA, Margison KD, Ghorbani P, LeBlond ND, O'Dwyer C, Nunes JRC, et al. Choline transport links macrophage phospholipid metabolism and inflammation. J Biol Chem [Internet]. 2018 Jul 7 [cited 2024 Apr 22];293(29):11600. Available from: /pmc/articles/PMC6065184/

55. Storck EM, Morales-Sanfrutos J, Serwa RA, Panyain N, Lanyon-Hogg T, Tolmachova T, et al. Dual chemical probes enable quantitative system-wide analysis of protein prenylation and prenylation dynamics. Nature Chemistry 2019 11:6 [Internet]. 2019 Apr 1 [cited 2024 Apr 24];11(6):552–61. Available from: https://www.nature.com/articles/s41557-019-0237-6

56. Kenwood BM, Weaver JL, Bajwa A, Poon IK, Byrne FL, Murrow BA, et al. Identification of a novel mitochondrial uncoupler that does not depolarize the plasma membrane. Mol Metab [Internet]. 2014 [cited 2024 Apr 24];3(2):114. Available from: /pmc/articles/PMC3953706/

57. Verberk SGS, de Goede KE, Gorki FS, van Dierendonck XAMH, Argüello RJ, Van den Bossche J. An integrated toolbox to profile macrophage immunometabolism. Cell Reports Methods [Internet]. 2022 Apr 4 [cited 2024 Apr 24];2(4). Available from: /pmc/articles/PMC9046227/

58. Corraliza IM, Campo ML, Soler G, Modolell M. Determination of arginase activity in macrophages: a micromethod. J Immunol Methods [Internet]. 1994 Sep 14 [cited 2024 Apr 24];174(1–2):231–5. Available from: https://pubmed.ncbi.nlm.nih.gov/8083527/

59. Grahame Hardie D. Regulation of fatty acid synthesis via phosphorylation of acetyl-CoA carboxylase. Prog Lipid Res. 1989 Jan 1;28(2):117–46.

60. Hay N, Sonenberg N. Upstream and downstream of mTOR. Genes Dev [Internet]. 2004 Aug 15 [cited 2024 Apr 29];18(16):1926–45. Available from: https://pubmed.ncbi.nlm.nih.gov/15314020/

61. Sag D, Carling D, Stout RD, Suttles J. Adenosine 5′-Monophosphate-Activated Protein Kinase Promotes Macrophage Polarization to an Anti-Inflammatory Functional Phenotype. The Journal of Immunology [Internet]. 2008 Dec 15 [cited 2024 Apr 30];181(12):8633–41. Available from: https://dx.doi.org/10.4049/jimmunol.181.12.8633

62. Egan DF, Shackelford DB, Mihaylova MM, Gelino S, Kohnz RA, Mair W, et al. Phosphorylation of ULK1 (hATG1) by AMP-activated protein kinase connects energy sensing to mitophagy. Science [Internet]. 2011 Jan 28 [cited 2024 Apr 29];331(6016):456–61. Available from: https://pubmed.ncbi.nlm.nih.gov/21205641/

63. Noda T, Ohsumi Y. Tor, a phosphatidylinositol kinase homologue, controls autophagy in yeast. Journal of Biological Chemistry [Internet]. 1998 Feb 13 [cited 2023 Dec 7];273(7):3963–6. Available from: http://www.jbc.org/article/S0021925817471572/fulltext

64. Lee JW, Park S, Takahashi Y, Wang HG. The Association of AMPK with ULK1 Regulates Autophagy. PLoS One [Internet]. 2010 [cited 2023 Dec 7];5(11):e15394. Available from: https://journals.plos.org/plosone/article?id=10.1371/journal.pone.0015394

65. Barbet NC, Schneider U, Helliwell SB, Stansfield I, Tuite MF, Hall MN. TOR controls translation initiation and early G1 progression in yeast. Mol Biol Cell [Internet]. 1996 [cited 2024 Apr 29];7(1):25. Available from: /pmc/articles/PMC278610/?report=abstract

66. Schneider-Poetsch T, Ju J, Eyler DE, Dang Y, Bhat S, Merrick WC, et al. Inhibition of eukaryotic translation elongation by cycloheximide and lactimidomycin. Nature Chemical Biology 2010 6:3 [Internet]. 2010 Jan 31 [cited 2024 May 21];6(3):209–17. Available from: https://www.nature.com/articles/nchembio.304

67. Schieke SM, Phillips D, McCoy JP, Aponte AM, Shen RF, Balaban RS, et al. The mammalian target of rapamycin (mTOR) pathway regulates mitochondrial oxygen consumption and oxidative capacity. J Biol Chem [Internet]. 2006 Sep 15 [cited 2024 May 1];281(37):27643–52. Available from: https://pubmed.ncbi.nlm.nih.gov/16847060/

68. Herzig S, Shaw RJ. AMPK: guardian of metabolism and mitochondrial homeostasis. Nat Rev Mol Cell Biol [Internet]. 2018 Jan 23 [cited 2024 Apr 30];19(2):121. Available from: /pmc/articles/PMC5780224/

69. Van den Bossche J, Baardman J, de Winther MPJ. Metabolic Characterization of Polarized M1 and M2 Bone Marrow-derived Macrophages Using Real-time Extracellular Flux Analysis. J Vis Exp [Internet]. 2015 Nov 28 [cited 2023 Dec 5];2015(105):53424. Available from: /pmc/articles/PMC4692751/

70. Sanne Verberk AG, de Goede KE, Gorki FS, AMH van Dierendonck X, Arg RJ, Verberk SG, et al. An integrated toolbox to profile macrophage immunometabolism. Cell Reports

Methods [Internet]. 2022 [cited 2023 Dec 5];2:100192. Available from: https://doi.org/10.1016/j.crmeth.2022.100192

71. Larsen S, Nielsen J, Hansen CN, Nielsen LB, Wibrand F, Stride N, et al. Biomarkers of mitochondrial content in skeletal muscle of healthy young human subjects. J Physiol [Internet]. 2012 Jul 1 [cited 2024 Apr 30];590(14):3349–60. Available from: https://onlinelibrary.wiley.com/doi/full/10.1113/jphysiol.2012.230185

72. Warburg O, Wind F, Negelein E. THE METABOLISM OF TUMORS IN THE BODY. J Gen Physiol [Internet]. 1927 Mar 3 [cited 2024 Apr 30];8(6):519. Available from: https://www.ncbi.nlm.nih.gov/pmc/articles/PMC2140820/

73. Mookerjee SA, Goncalves RLS, Gerencser AA, Nicholls DG, Brand MD. The contributions of respiration and glycolysis to extracellular acid production. Biochimica et Biophysica Acta (BBA) - Bioenergetics. 2015 Feb 1;1847(2):171–81.

74. Mathupala SP, Rempel A, Pedersen PL. Aberrant glycolytic metabolism of cancer cells: A remarkable coordination of genetic, transcriptional, post-translational, and mutational events that lead to a critical role for Type II hexokinase. J Bioenerg Biomembr [Internet]. 1997 [cited 2024 Apr 30];29(4):339–43. Available from: https://link.springer.com/article/10.1023/A:1022494613613

75. Xu H, Zhao Y, Zhao Q, Shi M, Zhang Z, Ding W, et al. Tuberous Sclerosis Complex 1 Deficiency in Macrophages Promotes Unclassical Inflammatory Response to Lipopolysaccharide In Vitro and Dextran Sodium Sulfate-Induced Colitis in Mice. Aging Dis [Internet]. 2022 Dec 12 [cited 2024 Apr 30];13(6):1875. Available from: /pmc/articles/PMC9662278/

76. Lee J, Ryu H, Ferrante RJ, Morris SM, Ratan RR. Translational control of inducible nitric oxide synthase expression by arginine can explain the arginine paradox. Proc Natl Acad Sci U S A [Internet]. 2003 Apr 15 [cited 2024 Apr 30];100(8):4843–8. Available from: https://pubmed.ncbi.nlm.nih.gov/12655043/

77. Wu G, Morris SM. Arginine metabolism: nitric oxide and beyond. Biochemical Journal [Internet]. 1998 Nov 15 [cited 2024 May 2];336(1):1–17. Available from: /biochemj/article/336/1/1/34432/Arginine-metabolism-nitric-oxide-and-beyond

78. Liew FY, Li Y, Moss D, Parkinson C, Rogers M V., Moncada S. Resistance to Leishmania major infection correlates with the induction of nitric oxide synthase in murine macrophages. Eur J Immunol [Internet]. 1991 Dec 1 [cited 2024 May 2];21(12):3009–14. Available from: https://onlinelibrary.wiley.com/doi/full/10.1002/eji.1830211216

79. Zweier JL, Samouilov A, Kuppusamy P. Non-enzymatic nitric oxide synthesis in biological systems. Biochimica et Biophysica Acta (BBA) - Bioenergetics. 1999 May 5;1411(2–3):250–62.

80. Liu W, Ye C, Cheng Q, Zhang X, Yao L, Li Q, et al. Macrophage Raptor Deficiency-Induced Lysosome Dysfunction Exacerbates Nonalcoholic Steatohepatitis. Cell Mol

Gastroenterol Hepatol [Internet]. 2019 Jan 1 [cited 2024 May 7];7(1):211. Available from: /pmc/articles/PMC6282883/

81. Kohlstedt K, Trouvain C, Namgaladze D, Fleming I. Adipocyte-derived lipids increase angiotensin-converting enzyme (ACE) expression and modulate macrophage phenotype. Basic Res Cardiol [Internet]. 2011 Mar [cited 2024 Apr 30];106(2):205–15. Available from: https://pubmed.ncbi.nlm.nih.gov/21116821/

82. Zhu L, Yang T, Li L, Sun L, Hou Y, Hu X, et al. TSC1 controls macrophage polarization to prevent inflammatory disease. Nature Communications 2014 5:1 [Internet]. 2014 Sep 1 [cited 2024 Apr 30];5(1):1–13. Available from: https://www.nature.com/articles/ncomms5696

83. Ai D, Jiang H, Westerterp M, Murphy AJ, Wang M, Ganda A, et al. Disruption of mammalian target of rapamycin complex 1 in macrophages decreases chemokine gene expression and atherosclerosis. Circ Res [Internet]. 2014 [cited 2024 Apr 30];114(10):1576–84. Available from: https://pubmed.ncbi.nlm.nih.gov/24687132/

84. Pan H, O'Brien TF, Zhang P, Zhong XP. The Role of Tuberous Sclerosis Complex 1 in Regulating Innate Immunity. The Journal of Immunology [Internet]. 2012 Apr 15 [cited 2024 May 9];188(8):3658–66. Available from: https://dx.doi.org/10.4049/jimmunol.1102187

85. Horman S, Browne GJ, Krause U, Patel J V., Vertommen D, Bertrand L, et al. Activation of AMP-activated protein kinase leads to the phosphorylation of elongation factor 2 and an inhibition of protein synthesis. Curr Biol [Internet]. 2002 Aug 20 [cited 2024 Jun 1];12(16):1419–23. Available from: https://pubmed.ncbi.nlm.nih.gov/12194824/

86. Tannahill G, Curtis A, Nature JA, 2013 undefined. Succinate is an inflammatory signal that induces IL-1β through HIF-1α. nature.comGM Tannahill, AM Curtis, J Adamik, EM Palsson-McDermott, AF McGettrick, G GoelNature, 2013•nature.com [Internet]. [cited 2024 May 9]; Available from: https://idp.nature.com/authorize/casa?redirect_uri=https://www.nature.com/articles/nature11986&casa_token=5Jjk9rH4VX4AAAAA:iEPyTmmkR-s_4SHiJ4Tcdy4JayU7VJ0vgA5CDgG6MU68eoMk2xh9z_oJoPviRuDoWi1GRK9xJcUJRBWFocY

87. Freemerman AJ, Johnson AR, Sacks GN, Milner JJ, Kirk EL, Troester MA, et al. Metabolic reprogramming of macrophages: Glucose transporter 1 (GLUT1)-mediated glucose metabolism drives a proinflammatory phenotype. Journal of Biological Chemistry [Internet]. 2014 Mar 14 [cited 2024 May 9];289(11):7884–96. Available from: http://www.jbc.org/article/S0021925820442917/fulltext

88. Feng D, Biftu T, Romero FA, Kekec A, Dropinski J, Kassick A, et al. Discovery of MK-8722: A Systemic, Direct Pan-Activator of AMP-Activated Protein Kinase. ACS Med Chem Lett [Internet]. 2018 Jan 11 [cited 2024 Jun 29];9(1):39–44. Available from: /pmc/articles/PMC5767883/

89. Haloul M, Oliveira ERA, Kader M, Wells JZ, Tominello TR, El Andaloussi A, et al. mTORC1-mediated polarization of M1 macrophages and their accumulation in the liver correlate with immunopathology in fatal ehrlichiosis. Scientific Reports 2019 9:1 [Internet]. 2019 Oct 1 [cited 2024 Jun 29];9(1):1–13. Available from: https://www.nature.com/articles/s41598-019-50320-y

90. Feng Y, Wu L. mTOR up-regulation of PFKFB3 is essential for acute myeloid leukemia cell survival. Biochem Biophys Res Commun [Internet]. 2017 Feb 5 [cited 2024 Jun 29];483(2):897–903. Available from: https://pubmed.ncbi.nlm.nih.gov/28082200/

91. Zhang Y, Kwok-Shing Ng P, Kucherlapati M, Chen F, Liu Y, Tsang YH, et al. A Pan-Cancer Proteogenomic Atlas of PI3K/AKT/mTOR Pathway Alterations. Cancer Cell [Internet]. 2017 Jun 12 [cited 2024 Jun 29];31(6):820-832.e3. Available from: https://pubmed.ncbi.nlm.nih.gov/28528867/

92. West MJ, Stoneley M, Willis AE. Translational induction of the c-myc oncogene via activation of the FRAP/TOR signalling pathway. Oncogene [Internet]. 1998 Aug 13 [cited 2024 Jun 29];17(6):769–80. Available from: https://pubmed.ncbi.nlm.nih.gov/9715279/

93. Hudson CC, Liu M, Chiang GG, Otterness DM, Loomis DC, Kaper F, et al. Regulation of hypoxia-inducible factor 1alpha expression and function by the mammalian target of rapamycin. Mol Cell Biol [Internet]. 2002 Oct 1 [cited 2024 Jun 29];22(20):7004–14. Available from: https://pubmed.ncbi.nlm.nih.gov/12242281/

94. Cunningham JT, Rodgers JT, Arlow DH, Vazquez F, Mootha VK, Puigserver P. mTOR controls mitochondrial oxidative function through a YY1-PGC-1alpha transcriptional complex. Nature [Internet]. 2007 Nov 29 [cited 2024 Jun 29];450(7170):736–40. Available from: https://pubmed.ncbi.nlm.nih.gov/18046414/

95. Diskin C, Pålsson-McDermott EM. Metabolic Modulation in Macrophage Effector Function. Front Immunol [Internet]. 2018 Feb 19 [cited 2024 Jun 1];9(FEB). Available from: https://pubmed.ncbi.nlm.nih.gov/29520272/

96. Yang Y, Jia Y, Ning Y, Wen W, Qin Y, Zhang H, et al. TAK1-AMPK Pathway in Macrophages Regulates Hypothyroid Atherosclerosis. Cardiovasc Drugs Ther [Internet]. 2021 Jun 1 [cited 2024 May 23];35(3):599–612. Available from: https://link.springer.com/article/10.1007/s10557-020-06996-w